SOME STUDIES IN ANALYTICAL ATOMIC SPECTROSCOPY

BELOW TWO HUNDRED NANOMETRES

by

MAURICE MARSHALL B.Sc., M.Sc.

ABSTRACT

This work describes an investigation of analytical atomic absorption spectroscopy below two hundred nanometres. Various possible atom cells are studied, and the inert gas separated nitrous oxide-acetylene flame is shown to be suitable for use at these wavelengths. The technique is applied to the direct determination of sulphur and phosphorus, and the results obtained are compared with those predicted theoretically. A number of possible improvements in the method are suggested.

ACKNOWLEDGEMENTS

The work described in this thesis was carried out in the Department of Chemistry, Imperial College of Science and Technology between October 1970 and October 1972. It is entirely original except where due reference is made and no part of the work has been submitted previously for any other degree.

I wish to thank my supervisor, Dr. G.F.Kirkbright, for his advice and encouragement, Professor T.S.West for his interest, and Mr. D.Alger for many helpful discussions. I also wish to acknowledge the assistance of Mr. R.Carter in producing Figure 1, and my wife Ann's unfailing patience in typing this work.

I am indebted to the Science Research Council and the British Steel Corporation for their support of this work under the C.A.P.S. scheme.

CONTENTS

CHAPTER 1

INTRODUCTION

Atomic absorption spectrometry was applied to the problems of analytical chemistry mainly as a result of the work of Walsh et al.(1, 2).

The technique is based upon the absorption by free atoms of light having wavelengths corresponding to electronic transitions between the discrete energy levels within the atom. Numerous accounts of the general theory of the subject have been given (3, 4, 5, 6, 7). More specialised topics such as the intensity, shape and width of spectral lines, together with the problems of self-absorption and self-reversal, have also been comprehensively covered (8, 9). A particularly useful exposition of the principles and practice of atomic absorption spectrometry has been given by L'vov (10).

Although the technique of atomic absorption spectrochemical analysis is now widely used, it has not been generally applied to a number of elements which have principal resonance lines whose wavelengths are less than two hundred nanometres. A list of these elements, and of the wavelengths of their principal resonance lines, is given in Table 1.

There are a number of difficulties which have largely prevented the application of atomic absorption spectrometry to the determination of these elements. Firstly, oxygen absorbs light of wavelengths below two hundred nanometres. This is illustrated by Figure 1, taken from L'vov (10).

Secondly, the transparency of silica decreases rapidly with shorter wavelength, and it is necessary to employ more expensive, less easily worked materials, such as calcium or lithium fluoride for optics.

Thirdly, there has been an apparent lack of a suitable means of generating the requisite atoms. This point does not, of course, apply to the noble gases, but is probably the most important factor in respect of the other elements considered.

Since the oxygen in the air, together with other common species such as water vapour, are opaque to the desired radiation,

Table 1

Elements with principal resonance lines of wavelength less than two hundred nanometres

Element	Wavelength, nm
Arsenic	197.3, 193.8, 189.0
Selenium	196.1
Mercury	184.9
Iodine	183.0, 178.3
Sulphur	182.6, 182.0, 180.7, 142.510, 129.566
Radon	178.6, 145.2
Phosphorus	178.7, 178.2, 177.5, 169.971, 167.461, 167.168
Carbon	165.7
Bromine	157.6, 148.9
Xenon	146.96, 129.56
Chlorine	138.0, 134.7
Oxygen	130.603, 130.487, 130.217
Krypton	123.584, 116.487
Hydrogen	121.567
Nitrogen	120.071, 120.02
Argon	106.666, 104.822
Fluorine	95.5, 95.2
Neon	74.372, 73.589
Helium	58.433

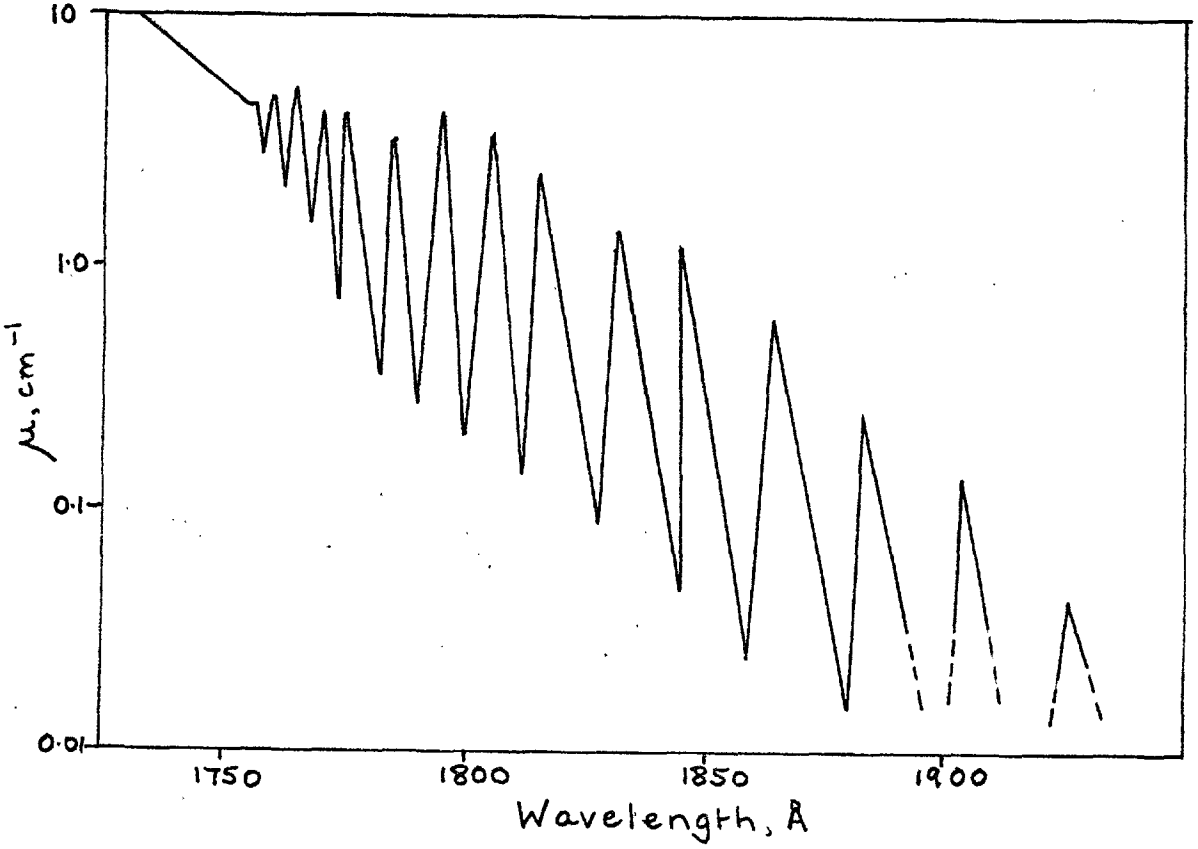

FIGURE 1

VARIATION OF THE COEFFICIENT OF OXYGEN ABSORPTION IN THE VACUUM REGION (1750-1950 Å)

they must be removed from the optical path. This may be achieved either by purging with an inert gas or by evacuation. Consequently the name "the vacuum ultra-violet" has come to be employed for the spectral region in question. This term is inaccurate and has sometimes led to confusion, but will be retained for its convenience.

These general problems of absorption by oxygen and the common optical materials in this spectral region were first overcome by Schumann. An interesting historical account is that of Lyman (11), whilst a useful review of modern techniques is given by Samson (12).

There is now no technical difficulty in building spectrometers which operate effectively in the vacuum ultra-violet. Additionally a number of light sources such as the hollow cathode lamp (9, 13) and the microwave excited electrodeless discharge lamp (14) are known to be suitable for production of the necessary spectral lines.

The major problem then, in the study of atomic absorption spectrochemical analysis in the vacuum ultra-violet, is the generation of the desired atoms.

Some early work on theoretical spectroscopy involved the elucidation of which spectral lines were in fact resonance lines. This was done by generating atoms in an evacuated tube which was either placed in a furnace or electrically heated. Fairly typical was a study of the absorption spectrum of iodine, carried out by J.H. McLeod (15). Figure 2 illustrates this worker's apparatus.

A modern development of the furnace technique is the graphite cuvette of L'vov (10, 16, 17). Figures 3 and 4 show the basic principle and general arrangement of the apparatus. The sample, placed on the electrode (A in Figure 3), is vaporised by electrical resistance heating of the electrode. The pulse of vapour which is produced passes into the cylindrical graphite cuvette (B in Figure 3). This cuvette is also electrically heated, so that the sample vapour may be maintained at a high temperature for appreciable periods of time. Provided the cell is at a sufficiently high temperature, the sample vapour will be dissociated into its constituent atoms, and the cell is there-

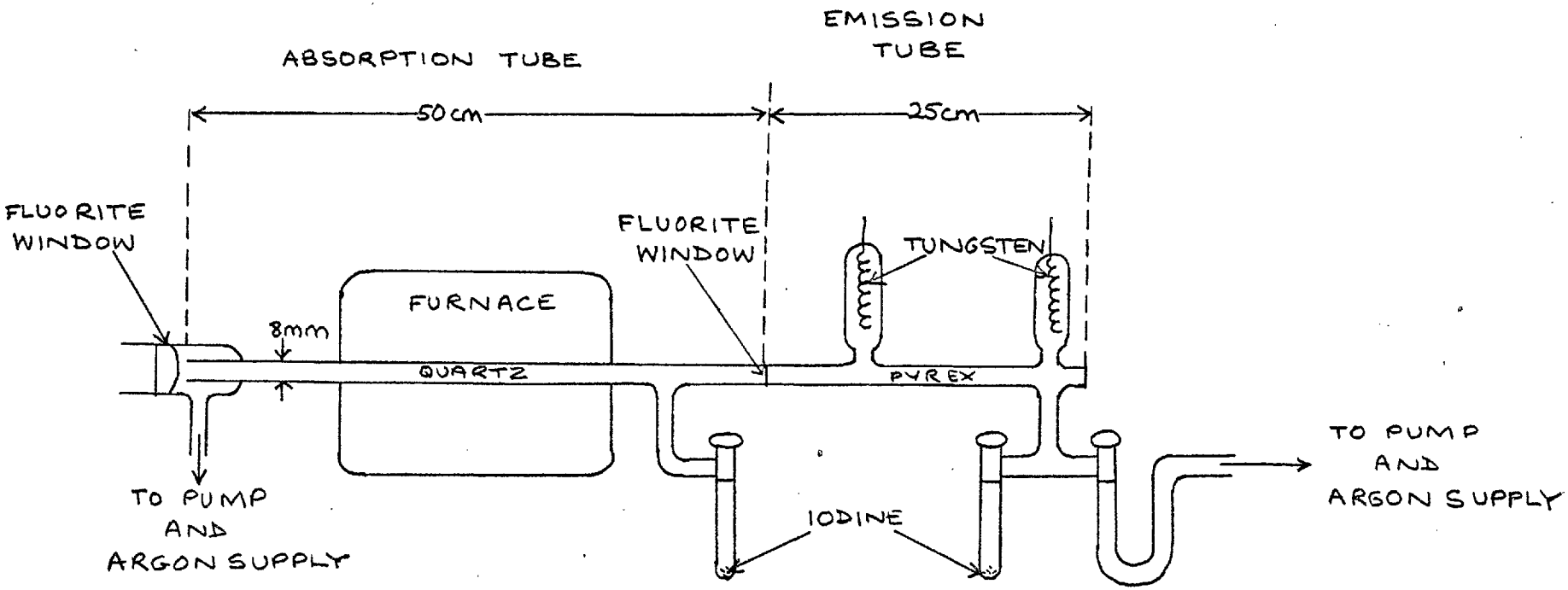

FIGURE 2

McLEOD'S APPARATUS

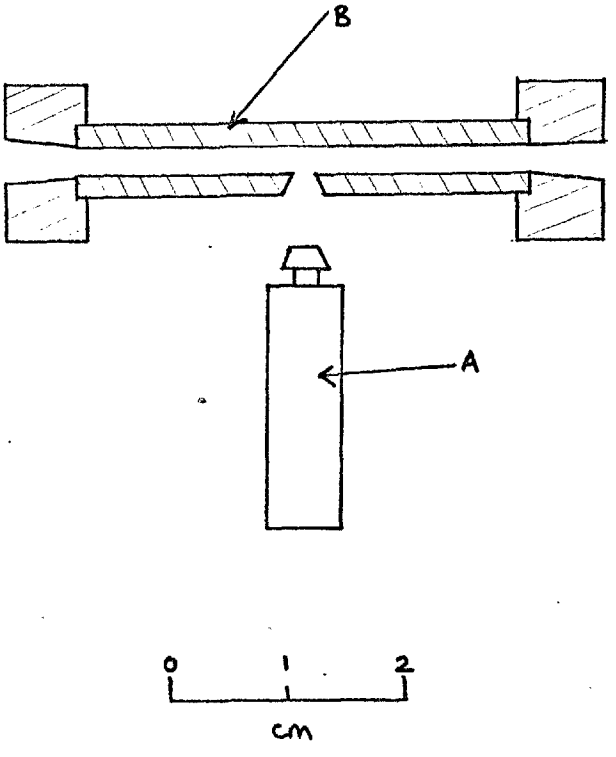

FIGURE 3

BASIC PRINCIPLE

OF L'VOV'S

GRAPHITE CUVETTE

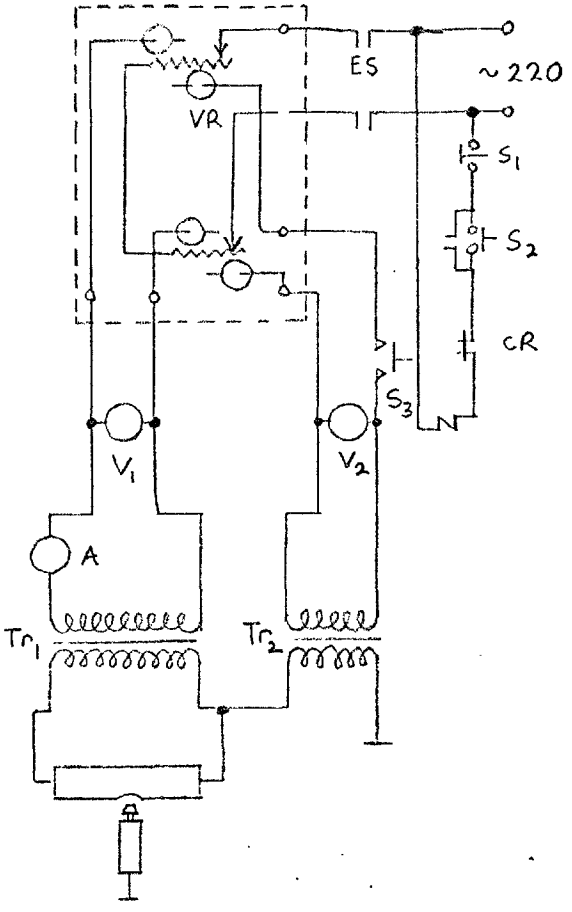

Tr_1	4 kW step-down transformer (220V/10V)
Tr_2	1 kW step-down transformer (220V/15V)
VR	Voltage regulator
ES	Electromagnetic switch
S_1, S_2	Switches for cuvette heating
S_3	Button switch for electrode heating
CR	Contact relay for control of water cooling system
V_1, V_2	Voltmeters (250V)
A	Ammeter (30 amp)

FIGURE 4

GENERAL ARRANGEMENT OF L'VOV'S GRAPHITE CUVETTE APPARATUS

fore useful for atomic absorption spectrometry. Atoms are lost from the cuvette by diffusion out of the ends; these losses due to diffusion are reduced by placing the cuvette in a chamber filled with inert gas (argon or nitrogen) at pressures up to ten atmospheres.

The particular excellence of this apparatus lies in the fact that the processes of sample vaporisation and dissociation of the vapour into atoms are separated; and that the atoms can be maintained at a controlled, uniform, high temperature for prolonged periods of time, up to 24.3 seconds in one experiment. Much higher absolute sensitivities are obtained with this technique than are possible with flame methods because the entire sample is conveyed into the analytical cell, rather than only a small fraction as in the case of most flames. In view of its theoretical and practical advantages, this apparatus probably represents the most important advance in analytical atomic absorption since the initial work of Walsh.

This very promising technique has been applied to the determination of a wide range of metals, and Khartsyzov and L'vov have also successfully used the method to determine mercury, iodine, sulphur and phosphorus (18). For this latter work the conventional argon filled cuvette assembly was used in conjunction with a vacuum monochromator and an electrodeless discharge source.

Massman (19) has developed a furnace type of non-flame cell which is somewhat similar to the design of L'vov; however certain modifications have been made, the most important being that the sample is vaporised by heating the furnace tube, rather than by an auxiliary electrode. Although slightly more convenient, this is a retrograde step as it increases the risk of matrix effects upon the determination.

Another type of non-flame atom cell which might be applicable in the vacuum ultra-violet is the carbon filament of West et al (20, 21) which is illustrated in Figure 5. The cell consists of a graphite filament which can be electrically heated. Small volumes (1-5μl) of sample solutions are placed in a depression in the centre of the filament. Electric current is then passed through the filament, causing it to rapidly attain

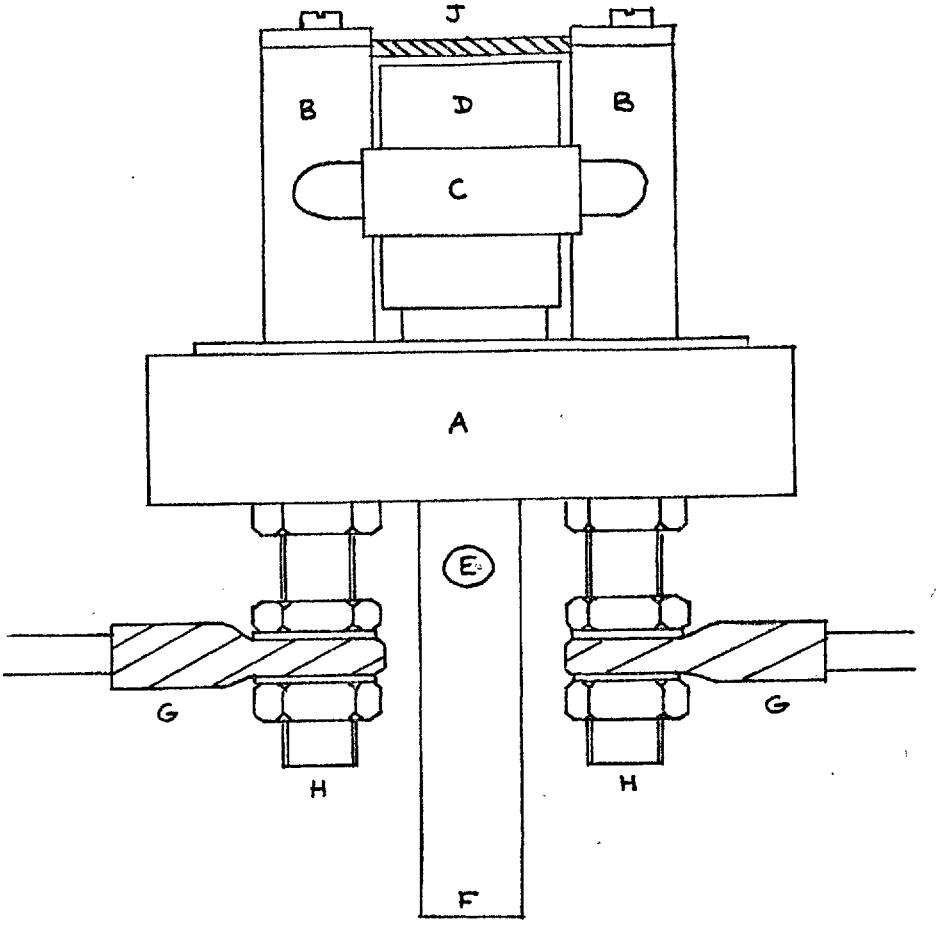

A	Base
B	Water-cooled electrodes
C	Water link between electrodes
D	Laminar-flow box
E	Inlet for shield gas
F	Support stem for reservoir
G	Transformer terminals
H	Water inlet and outlet
J	Filament

FIGURE 5

CARBON FILAMENT ATOM RESERVOIR

a very high temperature, up to 2000 or 2500°C. As the rod heats up the sample is vaporised, and in suitable circumstances the vapour is dissociated into atoms. Since the supply of energy to the atoms ceases immediately they leave the filament surface, the lifetime of the free atoms is very short, varying from a few milliseconds to a few hundred milliseconds. Additionally molecular species of high chemical stability may volatilise before they dissociate into atoms. The very short lifetime of the free atomic population makes it desirable to use high speed recording devices such as an oscilloscope (preferably of the storage type), a fast response recorder, or a transient selective integrator to detect the transient absorption signal.

Although the general design of this cell renders it very convenient for use in the vacuum ultra-violet, it is debatable whether such an essentially low energy system can reasonably be expected to dissociate and atomise very stable species such as the oxygen compounds of sulphur and phosphorus.

Radio-frequency excited plasmas in noble gases might also be considered as potential atom reservoirs for use in the vacuum ultra-violet. Apractical design of such a plasma torch is shown in Figure 6. The noble gas atoms (usually argon) are excited by means of radio-frequency energy supplied by inductive coupling via a work coil surrounding the torch body. Such a cell has more than adequate energy for the atomisation of non-metal species, but as has been demonstrated by the work of Fassel et al.(22) the high energy nature of these cells makes them more suitable for use in atomic emission rather than atomic absorption spectroscopy.

A considerable number of other designs of non-flame cell have been developed, all clearly inferior to that of L'vov. Details may be obtained from an excellent review of the subject by Kirkbright (23).

Conventional atomic absorption spectrophotometers employ a flame cell as the atom reservoir. This has the advantage of stability, simplicity and reliability. Flames are relatively free from memory effects, and have the merit that different flame mixtures can be used to vary the atomisation conditions. Equipment is relatively inexpensive and widely available. Sev-

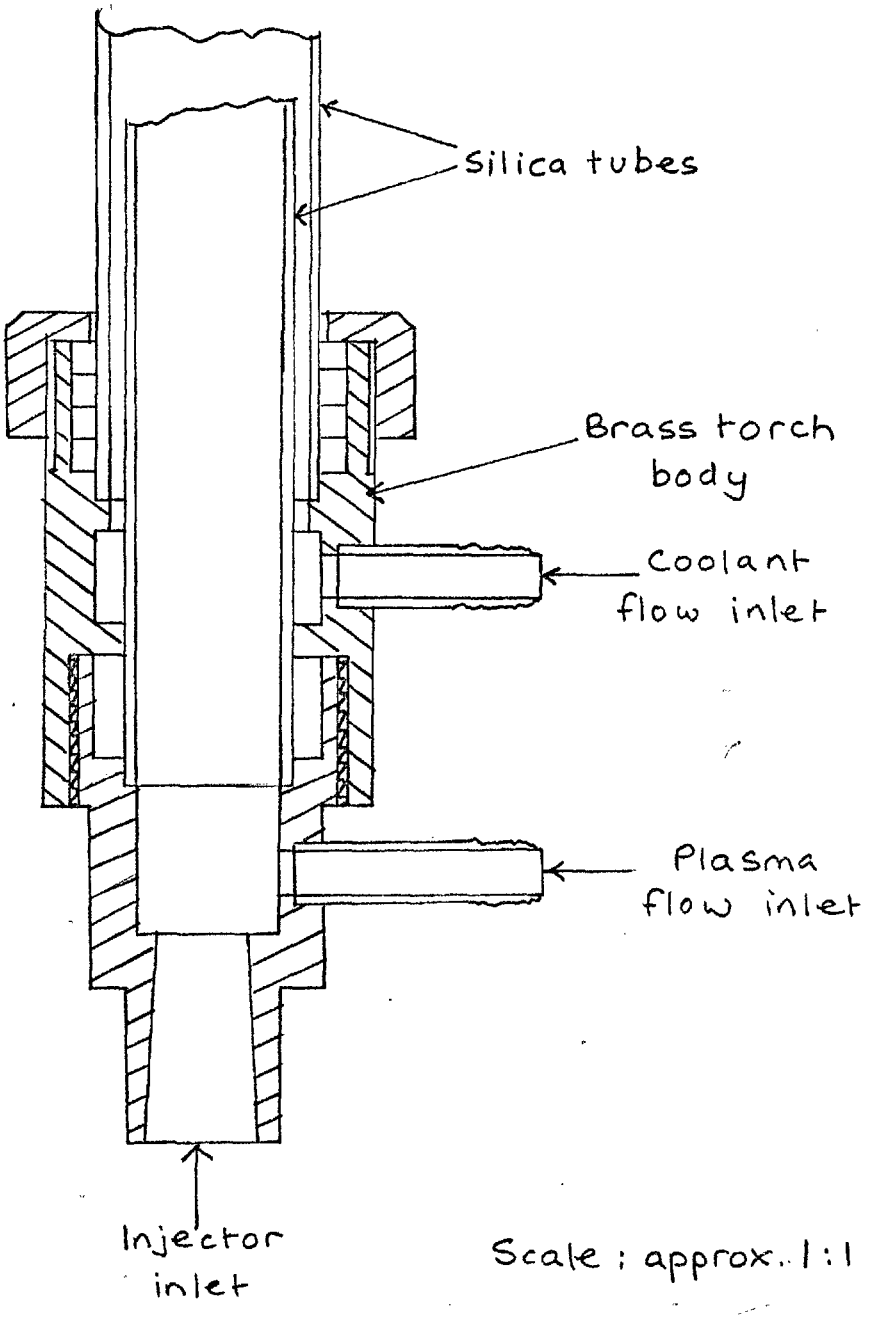

FIGURE 6

RF PLASMA TORCH

eral types of flame are in widespread use, e.g. the air-acetylene flame, the air-propane flame, the hydrogen-nitrogen diffusion flame and the nitrous oxide-acetylene flame. The ordinary air-propane and air-acetylene flames are opaque to short wavelengths; for instance a 10cm air-acetylene flame absorbs 70% of the incident radiation at 196nanometres (24). Slightly better transparency is exhibited by the hydrogen-nitrogen diffusion flame, which has been successfully employed for the determination of arsenic and selenium (25). Unfortunately the analytical response in this rather cool flame is often interfered with by the other species present, and this limits its utility.

Previous workers have assumed that:

1. Flames used for atomic absorption spectrometry require oxygen to support combustion.
2. Therefore they must contain oxygen.
3. Oxygen (and especially hot molecular oxygen) absorbs very strongly in the spectral region below 200 nanometres.
4. Therefore flames must also absorb such radiation, and cannot be used successfully for determinations at short wavelengths.

Further consideration shows that proposition 2 does not inevitably follow from the premise of statement 1. Therefore the argument as a whole could be invalid, and it might be possible to extend the spectral range of flame cells.

Essentially, the point is that the oxygen necessary for combustion in a flame is consumed by reaction with the fuel. Why then should a flame contain any free oxygen?

Two reasons are immediately apparent:

1. The reactions occurring between fuel and oxidant in a flame are a complex series of equilibria and might result in an appreciable residual partial pressure of free oxygen.
2. Flames are normally burnt in the open air. Oxygen from the surrounding atmosphere could possibly enter the flame, so decreasing its transparency. This is known as "air entrainment".

Air entrainment might be prevented by surrounding the flame with either a solid wall, e.g. a silica tube (26) or a blanket of oxygen-free inert gas(27). The latter technique is rather

safer. Such flames are known as "separated flames".

Having resolved the difficulty of air entrainment, the question of the composition of the flame mixture itself still remains to be answered.

The inter-conal zone of the fuel rich nitrous oxide-acetylene flame (see Figure 7) has been used for the determination of elements forming refractory oxides. The remarkably efficient atomisation of these elements has been explained in terms of the presence of the very strongly reducing cyanogen species (28, 29, 30) in this region of the flame, popularly known as the "red feather zone".

Kirkbright et al. have demonstrated that inert gas separation of the fuel rich nitrous oxide-acetylene flame further increases its reducing nature. These workers have successfully used this flame for the determination of arsenic and selenium (31), finding a high transparency at these wavelengths.

The general discussion above leads to consideration of three possible means, other than the L'vov furnace, of extending the range of atomic absorption spectrochemical analysis into the vacuum ultra-violet:

1. The carbon filament atom reservoir.
2. The hydrogen-nitrogen diffusion flame.
3. The nitrogen separated fuel rich nitrous oxide-acetylene flame.

In order to study the merits and demerits of these three proposals, the atomic absorption spectrochemical analysis of sulphur and phosphorus was investigated.

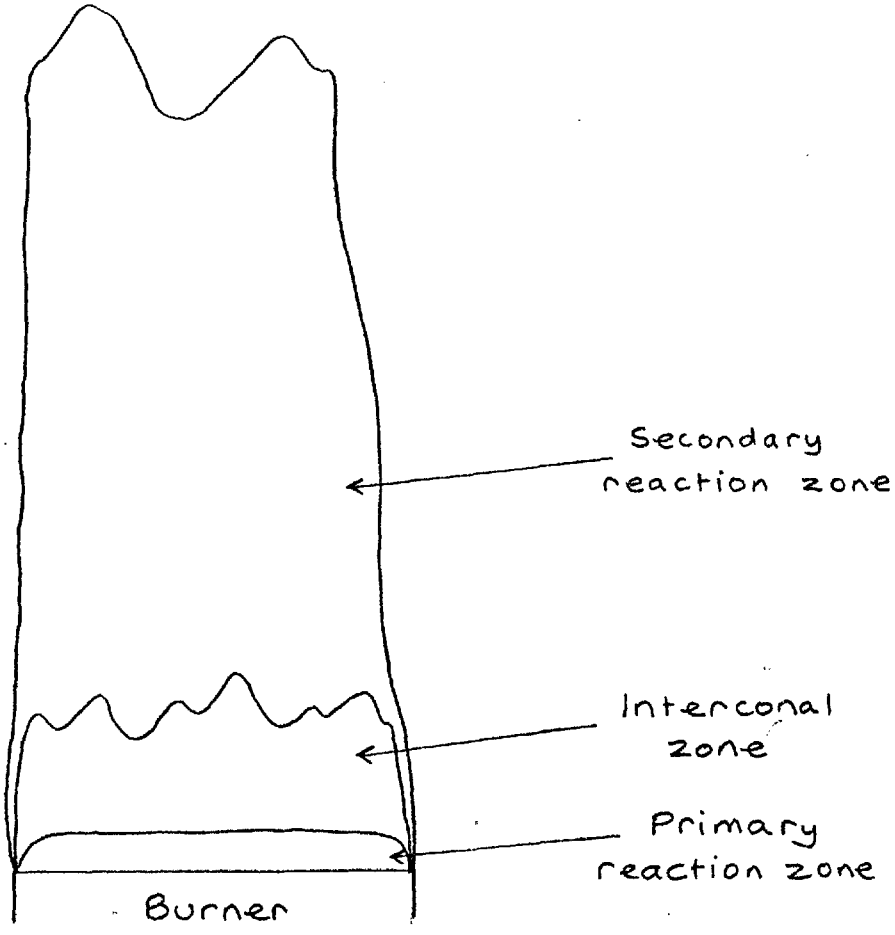

FIGURE 7

STRUCTURE OF A FUEL RICH

NITROUS OXIDE – ACETYLENE FLAME

CHAPTER 2

ATOMIC ABSORPTION SPECTROMETRY OF SULPHUR

2.1 Introduction

The atomic spectrum of sulphur is complex, containing many lines which originate in or near the ground state. This complexity is encouraged by the occurrence of two low lying energy levels at 397 cm^{-1} and 574 cm^{-1} above the ground state (32). A better appreciation of the situation may be obtained from the Grotrian diagram shown in Figure 8 (33).

Most of these resonance lines have low oscillator strengths, and consequently are of no interest for purposes of absorption spectrometry. A selection of potentially useful lines, having f-values greater than 0.1, together with relevant data, is given in Table 2. From the values given it is evident that the most sensitive absorption line should be 142.510 nm, followed by 180.734 nm and 129.566nm.

Khartsyzov and L'vov (10, 18) were able to determine sulphur by absorption measurements, using a graphite cuvette as the atom reservoir. They stated that the best sensitivity was obtained at the 180.7 nm line; however it is not clear whether they were able to study the lower lying lines. These workers found that a cuvette temperature of 1900°C was satisfactory.

Amos et al (34) attempted to determine sulphur at the $^3P-^3S^o$ lines using a carbon rod atomiser but were unsuccessful.

The only other reported observation of atomic absorption of sulphur was that of Taylor, Gibson and Skogerboe (35). These workers used a microwave plasma to produce sulphur atoms, and were able to observe absorption from excited states at the 216.89 nm line.

It was decided that study of the atomic absorption spectrometry of sulphur would be undertaken, using three of the possible atom reservoirs, viz:

the carbon filament atom reservoir (CFAR) (20),

the hydrogen-nitrogen diffusion flame,

the separated nitrous oxide-acetylene flame.

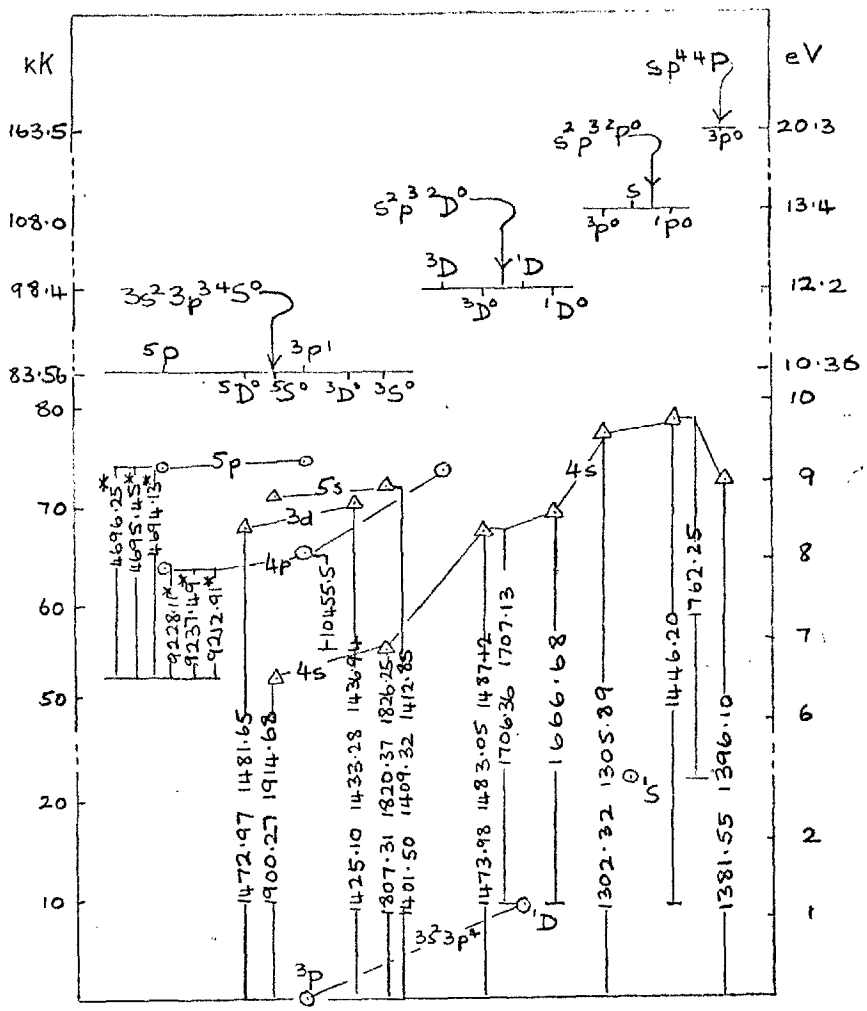

FIGURE 8

GROTRIAN DIAGRAM

FOR SULPHUR

Table 2

Some important resonance lines of the sulphur atom (32)

Transition array	$3p^4-3p^3(^2P^o)4s''$							
Multiplet	$^3P-^3P^o$		$^3P-^3D^o$			$^3P-^3S^o$		
Wavelength (nm)	129.566	130.589	142.510	143.333	143.701	180.734	182.036	182.626
Lower energy level E_i cm^{-1}	0	574	0	397	574	0	397	574
Upper energy level E_k cm^{-1}	77181	77151	70171	70167	70166	55331	55331	55331
Statistical weight g_i	5	1	5	3	1	5	3	1
Statistical weight g_k	5	3	7	5	3	3	3	3
Oscillator strength f_{ik}	0.12	0.13	0.15	0.14	0.19	0.12	0.11	0.11
Uncertainty in f_{ik} value	<50%	<50%	<50%	<50%	<50%	<25%	<25%	<25%
Transition probability A_{ki} (10^8 sec^{-1})	4.8	1.7	3.5	2.7	2.0	4.1	2.2	0.73

2.2 Experimental

Monochromator

An E796 vacuum polychromator (Hilger and Watts, Ltd., London) (36) was modified by removal of the spark housing, and attachment of a table carrying an optical bar to permit its use for atomic absorption measurements.

The instrument was originally designed to measure simultaneously the carbon, sulphur and phosphorus contents of steels by spark emission. Light emitted by the sample was dispersed by a train of fluorite prisms, and a characteristic wavelength of each element focussed on one of four photomultipliers. The four channels of the particular instrument employed for this work had been preset to the carbon 165.7 nm, iron 171.3 nm, phosphorus 178.3 nm and sulphur 180.7 nm lines (37). A degree of wavelength adjustment was provided by means of a "profile" control, consisting of a micrometer attached to the entrance slit, which moved the slit across the optical axis of the machine. This profile control gave a free spectral range of approximately ± 1 nm on each channel, which unfortunately was insufficient to allow observation of sulphur lines other than the 180.7 nm line.

The spectrometer was evacuated to a pressure of 0.15 to 0.20 torr.

Readout and detection system

The output from the photomultiplier (EMI 6256B, EMI Electronics, Ruislip, U.K.) was amplified by a battery operated microammeter (RCA Model WV 84C) and then displayed either at its meter or on a potentiometric chart recorder (Servoscribe Model 211R, Smiths Industries, U.K.).

Carbon filament atom reservoir

This was similar to that described by West and Williams (20). Light from the spectral source was restricted by a diaphragm into a narrow beam which then passed across to the carbon filament and into the monochromator. The optical path was purged with nitrogen.

Hydrogen-nitrogen diffusion flame

A 1 cm round burner was fitted to the indirect nebuliser used for the separated flame work. Solutions were nebulised on nitrogen. Otherwise the apparatus was similar to that described below.

Nitrogen separated nitrous oxide-acetylene flame

The instrumental assembly is shown in Figure 9.

The burner employed was a watercooled 7 cm nitrous oxide-acetylene slot burner (Beckman-RIIC, Glenrothes, Scotland) with facility for separation of the flame by inert gas shielding (27). This burner was mounted on the indirect nebuliser from a commercial atomic absorption spectrometer (Perkin-Elmer Corp., Norwalk, Conn., Model 290B). Sample solutions were nebulised on nitrous oxide (8.2 l/min) and the aqueous sample uptake rate was 6.5 ml/min. The optimum acetylene flow rate was 4.2 l/min, and the flame was separated by nitrogen (55 l/min). Glass tubing of 25 mm diameter, fitted with optically flat fused silica windows of the same diameter, was placed between the source and lens (25 mm diameter, 63 mm focal length) used to focus the radiation into the flame, and also between this lens and the flame, and the flame and collimating lens of the monochromator. These tubes were purged with nitrogen (1 to 3 l/min) to provide a light path appreciably more transparent than the atmosphere, and assisted the collection of as much radiant energy as possible at the monochromator.

Sulphur electrodeless discharge lamp

The sulphur electrodeless discharge lamp (EDL) was made from silica tubing (8mm bore, 1 mm thickness) to form a bulb of length 60 mm containing about 1 mg of sublimed sulphur and an argon filler gas pressure of 3 torr. The lamp was operated in a 3/4 wave resonant cavity (Model 210L, Electromedical Supplies, Wantage, U.K.) powered by a 2450 MHz Microtron Mk II microwave generator (Electromedical Supplies, Wantage, U.K.) at 20 watts using a -3 dB attenuator, so that the effective power to the lamp was 10 watts.

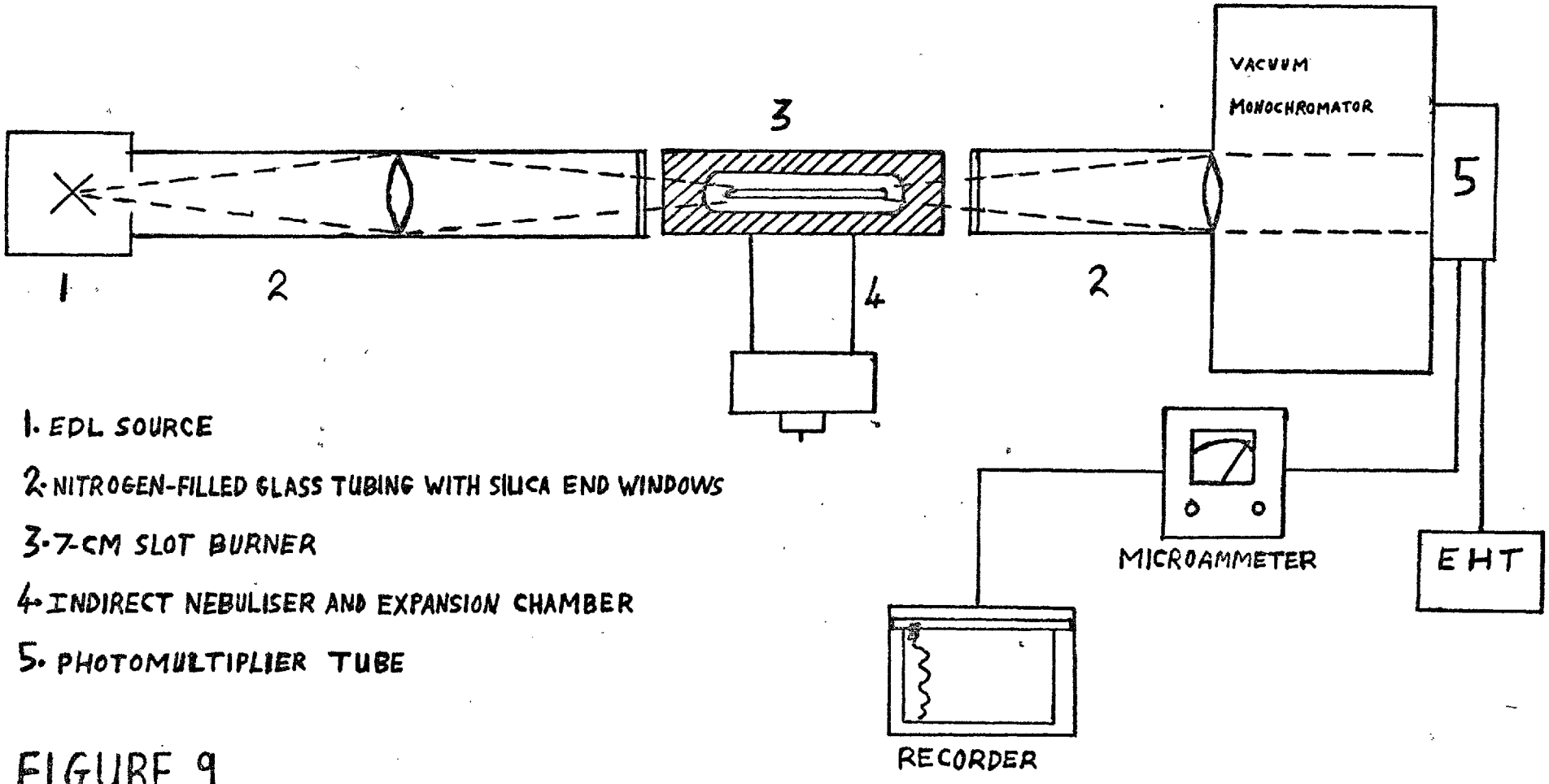

1. EDL SOURCE
2. NITROGEN-FILLED GLASS TUBING WITH SILICA END WINDOWS
3. 7-CM SLOT BURNER
4. INDIRECT NEBULISER AND EXPANSION CHAMBER
5. PHOTOMULTIPLIER TUBE

FIGURE 9

INSTRUMENTAL ASSEMBLY USING DC DETECTION

Reagents

A stock solution containing 5000 mg/l sulphur was prepared by dissolving analytical reagent grade potassium sulphate (27.17g) in 1 litre of distilled water. Working standards were prepared by dilution of the solution, as necessary.

The potassium thiocyanate, sodium thiosulphate and thiourea solutions were also prepared from analytical reagent grade chemicals. Solutions of dibenzyldisulphide, t-butyldisulphide, t-butylsulphide, or thiophen in methyl iso-butyl ketone were prepared from chemicals of known purity.

Stock solutions of the diverse ions used in the interference studies were prepared from analytical reagent grade salts of the elements.

2.3 Results for the carbon filament atom reservoir

When the carbon rod was dosed with small amounts of sulphur, either as solutions of compounds or as elemental sulphur, an absorption was obtained at the 180.7 nm sulphur line which persisted for several minutes after the rod had been fired. It seemed obvious that this was the result of molecular absorption and that the energy supplied by the CFAR to the sample was insufficient to cause dissociation into sulphur atoms.

In view of the experience of Amos et al (34), this work was discontinued.

2.4 Results for the hydrogen-nitrogen diffusion flame

Absorption at the 180.7 nm sulphur line was observed when sulphuric acid solution was sprayed into a hydrogen-nitrogen diffusion flame. No absorbance was obtained when strong solutions of phosphoric acid, sodium chloride or sodium iodide were sprayed into the flame and no flame emission was detected. Experiments were made, varying the hydrogen flow rate whilst spraying a constant strength sulphuric acid solution, and noting the effect on the absorbance. At low hydrogen flow rates, when the flame was presumably very cool, an intense blue emission due to S_2 molecules was observed, with little absorption at

180.7 nm. At higher hydrogen flow rates, when the flame was presumably hotter, the S_2 molecular emission disappeared and the absorption at 180.7 nm increased.

A hydrogen flow rate of 4 l/min and a nitrogen flow rate of 2.5 l/min were found satisfactory for absorption measurements.

The absorbance produced was found to be linearly proportional to the concentration of sulphur. Figure 10 shows a calibration curve for sulphuric acid obtained before the system was fully optimised.

Measurements were made to establish the percentage transmission of the hydrogen-nitrogen diffusion flame; Figure 11 is a reproduction of a recorder trace showing the flame transmission to be about 46% of that of air.

It was also decided to investigate the response of the system to sulphur present in different forms. Accordingly, solutions of different sulphur species, each containing 1000 mg/l, were sprayed, and the absorption signal recorded. Figure 12 is a reproduction of the trace obtained. As can be seen, different sulphur species give different responses for the same sulphur content. No absorbance was obtained from potassium sulphate solution; the response from sulphuric acid (not shown in Figure 12) was less than that from sodium thiosulphate.

2.5 Discussion of atomic absorption spectroscopy in the hydrogen-nitrogen diffusion flame

It seems clear that the absorption obtained at 180.7nm was due to the presence of sulphur atoms in the flame. The low sensitivity and susceptibility to interference effects (resulting from the low flame temperature) make it improbable that the hydrogen-nitrogen diffusion flame could be used as an atom reservoir for the determination of sulphur in real situations. However it might be possible to enhance the sensitivity obtained with the hydrogen-nitrogen diffusion flame by converting the sulphur present in a sample into hydrogen sulphide, and then introducing the latter into the flame. This process, analogous to those suggested in the literature for arsenic and selenium (38), might also be applicable to phosphorus.

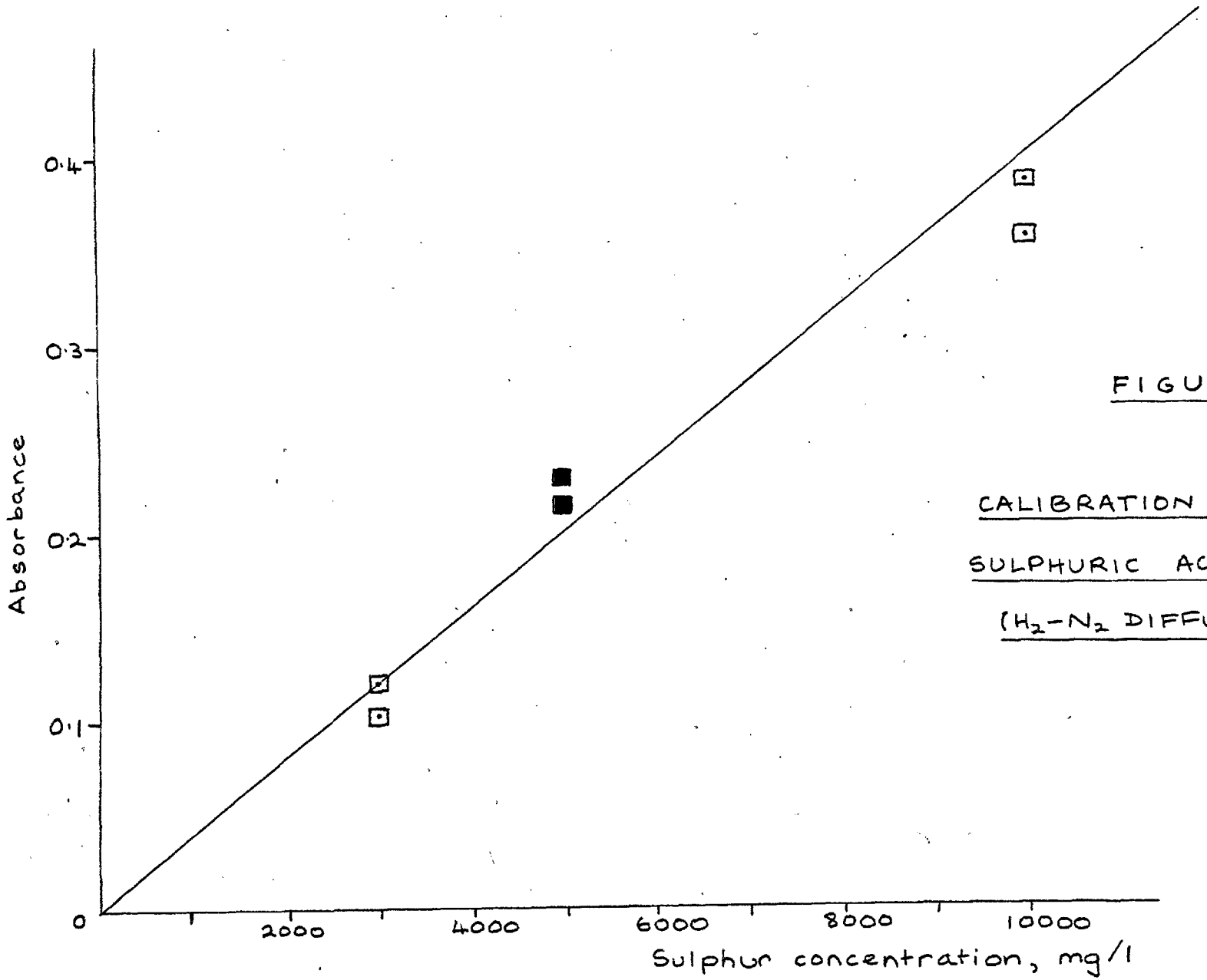

FIGURE 10

CALIBRATION CURVE FOR SULPHURIC ACID AT 180·7NM (H_2-N_2 DIFFUSION FLAME)

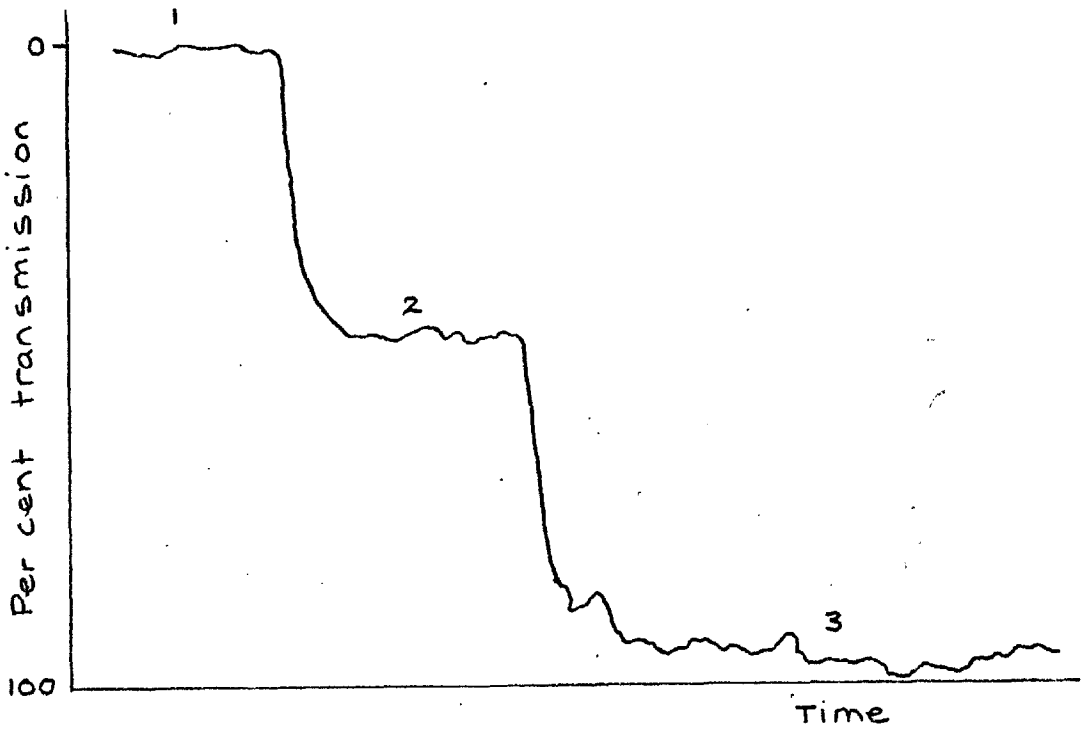

1 Zero transmission
2 H_2-N_2 diffusion flame
3 Air

FIGURE II

TRANSMISSION OF A 1 CM

H_2-N_2 DIFFUSION FLAME

AT 180·7NM RELATIVE TO AIR.

FIGURE 12

RESPONSE FROM DIFFERENT SPECIES AS SOLUTIONS OF 1000 mg/l SULPHUR IN THE H_2–N_2 DIFFUSION FLAME

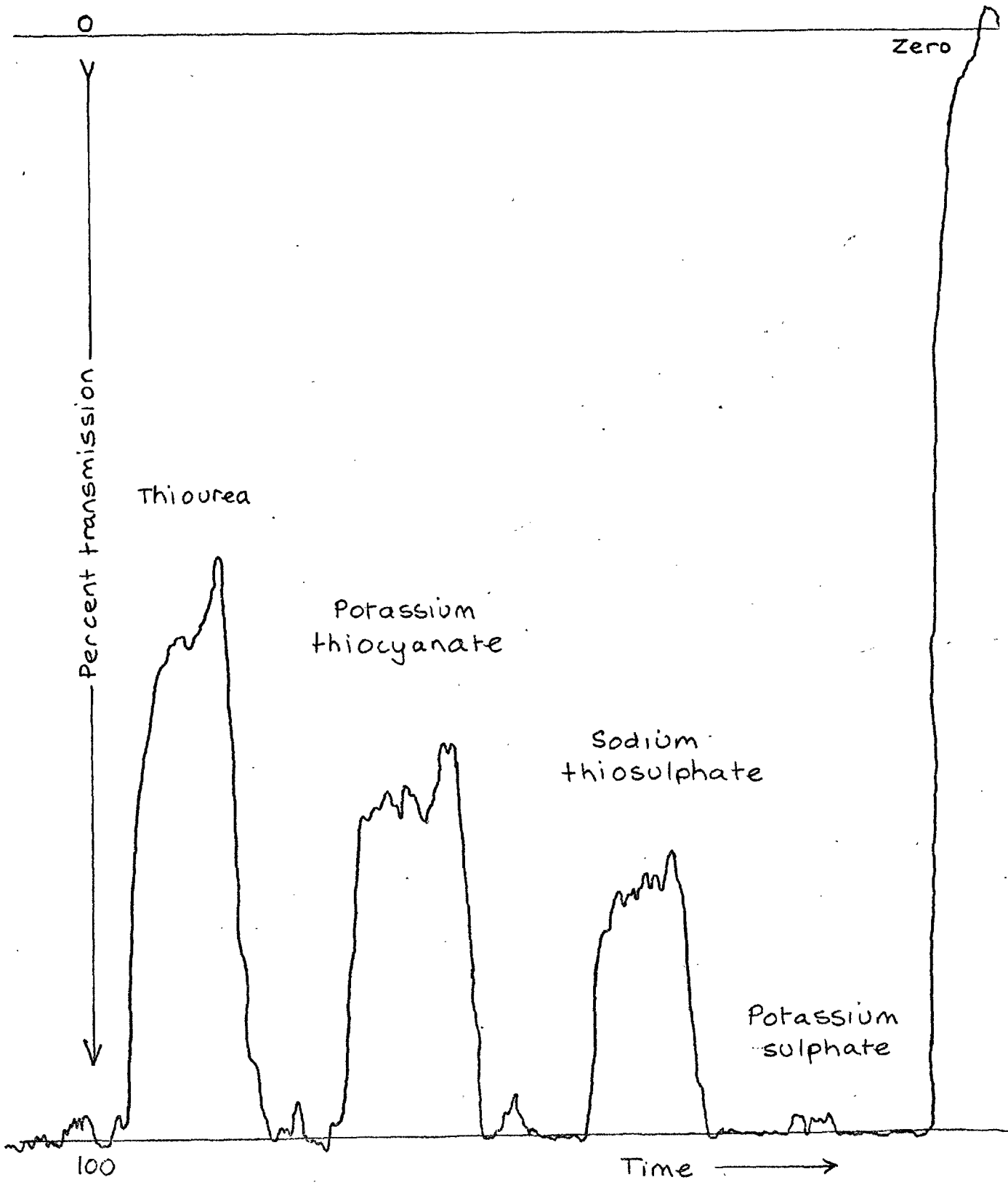

The improved sensitivity is due to two main factors:

1. the improved efficiency of transfer of sample into the flame,
2. the increased ease of dissociation of the non-metal hydrides compared to their diverse other compounds.

The differing responses obtained from different sulphur species are very similar to the interference effects noted by Thompson (39) in work on the emission spectrum of S_2 molecules. It would seem likely, from the fact that the interferences are common to both formation of S_2 and S atoms, that it is the initial dissociation of the original compounds into simpler species which is hindered, rather than any later step in the dissociation process.

Simultaneous observation of the S_2 molecular emission and the S atomic absorption should yield useful information on the various equilibria involved, and in view of the widespread use of cool flame sulphur detectors in gas chromatography, such theoretical information would be of considerable interest.

2.6 Transmission characteristics of the separated nitrous oxide-acetylene flame

The red feather zone of the separated nitrous oxide-acetylene flame transmitted appreciable amounts of 180.7 nm radiation. Figure 13 shows a typical recorder tracing of the effect on the transmission of the source radiation with and without the flame ignited and with and without nitrogen separation of the flame. Using the assembly illustrated in Figure 9, and setting the amplifier gain to 100% transmission while the flame is unignited and only the nitrogen gas is flowing, it is evident from Figure 13 that the transmission of the atmosphere is only 25% relative to that of nitrogen (2 in Figure 13). The transmission of the unshielded air-acetylene and nitrous oxide-acetylene flames is even less being approximately 3% and 7% respectively (3 and 4 in Figure 13), while that of the nitrogen separated nitrous oxide-acetylene flame is very substantial (5 in Figure 13). The recorded transmission of the flame at the optimum fuel flow rate for sulphur is 64% of that of nitrogen alone,

FIGURE 13

TRANSMISSION OF 180·7NM RADIATION BY FLAME SYSTEM

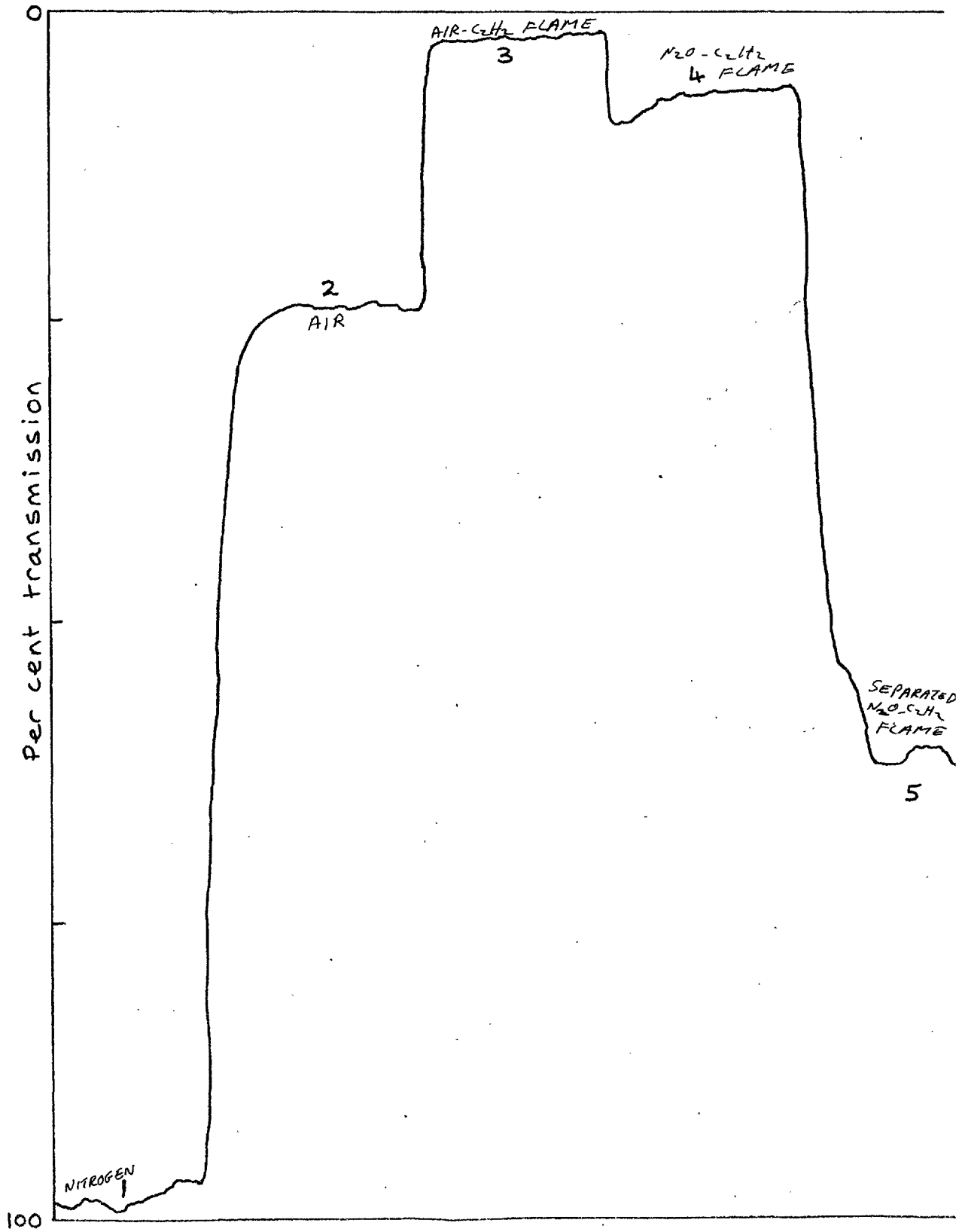

and approximately 2.5 times greater than that of air. No background emission from the flame was observed.

Figure 14 shows the effect of the variation in acetylene flow rate on the flame background transmission at 180.7nm. It is apparent that the acetylene flow rate employed should be closely controlled. Maximum flame transparency occurs when a slightly fuel-rich flame is employed, between 4.3 and 4.5 l/min of acetylene with a nitrous oxide flow rate of 8.2 l/min. The decreased transmission in the leaner flame may be attributed to the presence of absorbing oxygen species in the interconal zone, while that of the richer incandescent flame may be due to absorption by excess gaseous or particulate carbon species in this zone. The fuel flow rate which was found here to produce the greatest sensitivity (for 1% absorption) was 4.2 l/min of acetylene, slightly less than that necessary for maximum flame transmission. As mentioned earlier, at this flow rate the flame transmission was 64% of that of nitrogen alone.

2.7 Effect of operating power on sensitivity and source stability

The variation of the sensitivity obtained during the determination of sulphur with the operating power of the EDL was investigated. The lowest attainable operating power was found to produce the highest sensitivity; with the lamps used in this study this corresponded to approximately 10 watts input to the 3/4 wave cavity. As the operating power was increased the sensitivity decreased, an effect probably caused by excessive pressure and self-absorption broadening of the 180.7 nm line at higher power.

Better stability of the EDL was obtained by fitting a -3dB attenuator between the microwave power supply and the resonant cavity. This allowed the microwave generator to be operated on higher powers, giving greater output stability, and also minimised fluctuations due to "feedback" from the EDL to the power supply.

FIGURE 14

EFFECT OF VARIATION IN ACETYLENE FLOW RATE

ON FLAME BACKGROUND TRANSMISSION AT 180.7 NM

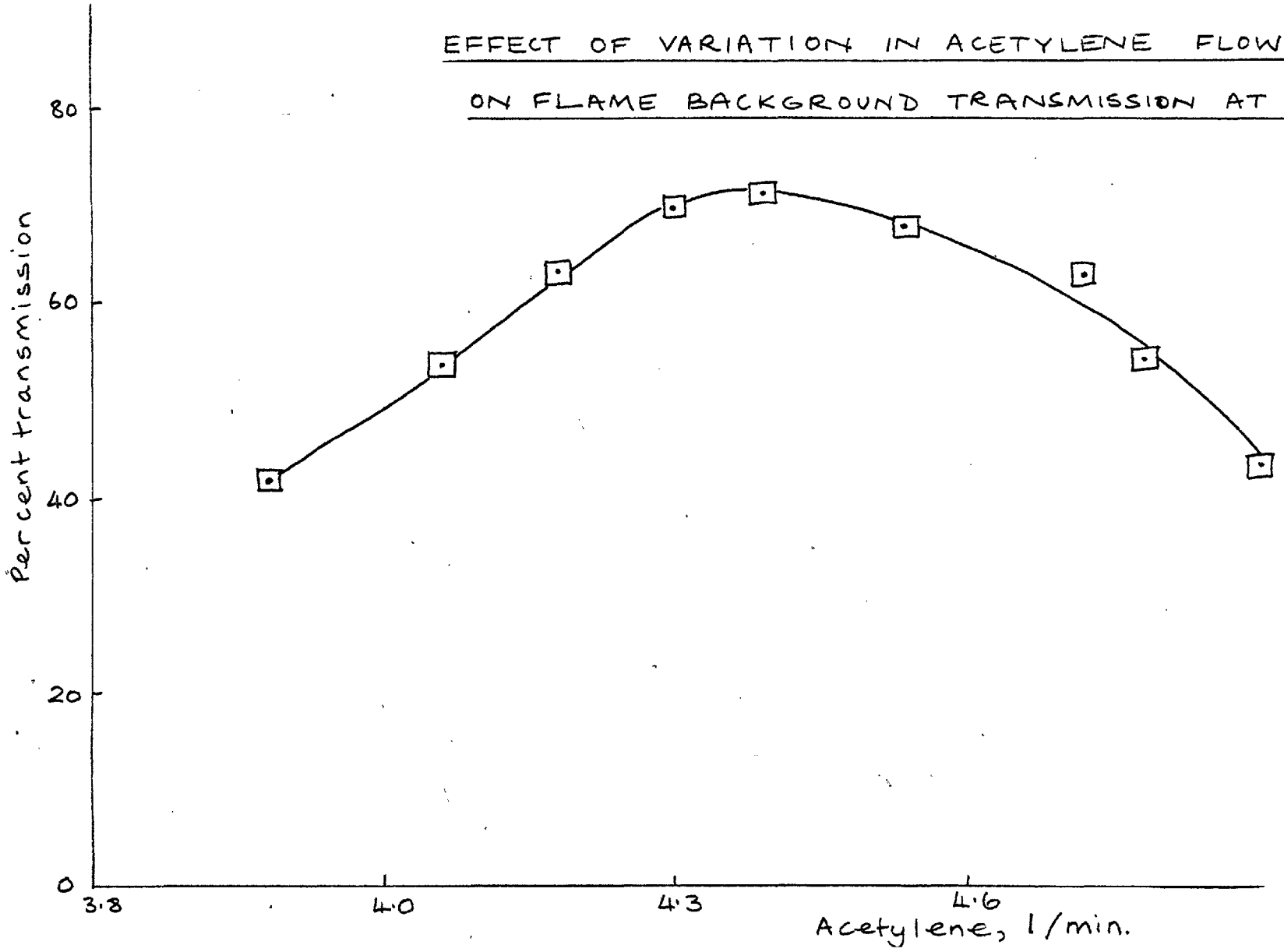

2.8 Sensitivity, detection limits and interferences

With the optimum operating conditions for the experimental assembly used in this work the sensitivity values (for 1% absorption) and detection limits shown in Table 3 were obtained for sulphur as sulphate in aqueous solution and sulphur as thiourea in ethanolic solution.

Table 3

Sensitivities and detection limits obtained

Analyte	Sensitivity (mg/l / 1% absorption)	Detection limit (mg/l)
Sulphur as K_2SO_4 in water	9.0	30
Sulphur as thiourea in ethanol	4.4	12

The 1% absorption sensitivity values were obtained from calibration curves. These were found to be linear for sulphate in water between 50 and 700 mg/l (Figure 15), and for thiourea in ethanolic solution between 20 and 500 mg/l (Figure 15). The detection limits are defined to correspond to that concentration of sulphur in each medium which produces a signal equal to twice the standard deviation in the signal noise obtained near the limit of detection.

No significant chemical or physical interference effect was observed in the absorbance signal produced by 200 mg/l sulphur in aqueous medium at 180.7 nm in the presence of 50-fold weight excesses of the following ions:

Al^{3+}, Cu^{2+}, K^{+}, Mg^{2+}, Mn^{2+}, Na^{+}, Ni^{2+}, Zn^{2+},

fluoride, phosphate, chloride, bromide, iodide.

As is evident from Figure 16, the introduction of the sulphur into the flame as thiosulphate, thiocynate or thiourea in aqueous solution resulted in similar 1% absorption sensitivities and detection limits to those obtained for sulphur introduced as sulphate in aqueous medium. The enhancement of sensitivity

FIGURE 15

CALIBRATION CURVES FOR SULPHATE IN WATER AND THIOUREA IN ETHANOL IN THE $N_2O-C_2H_2$ FLAME

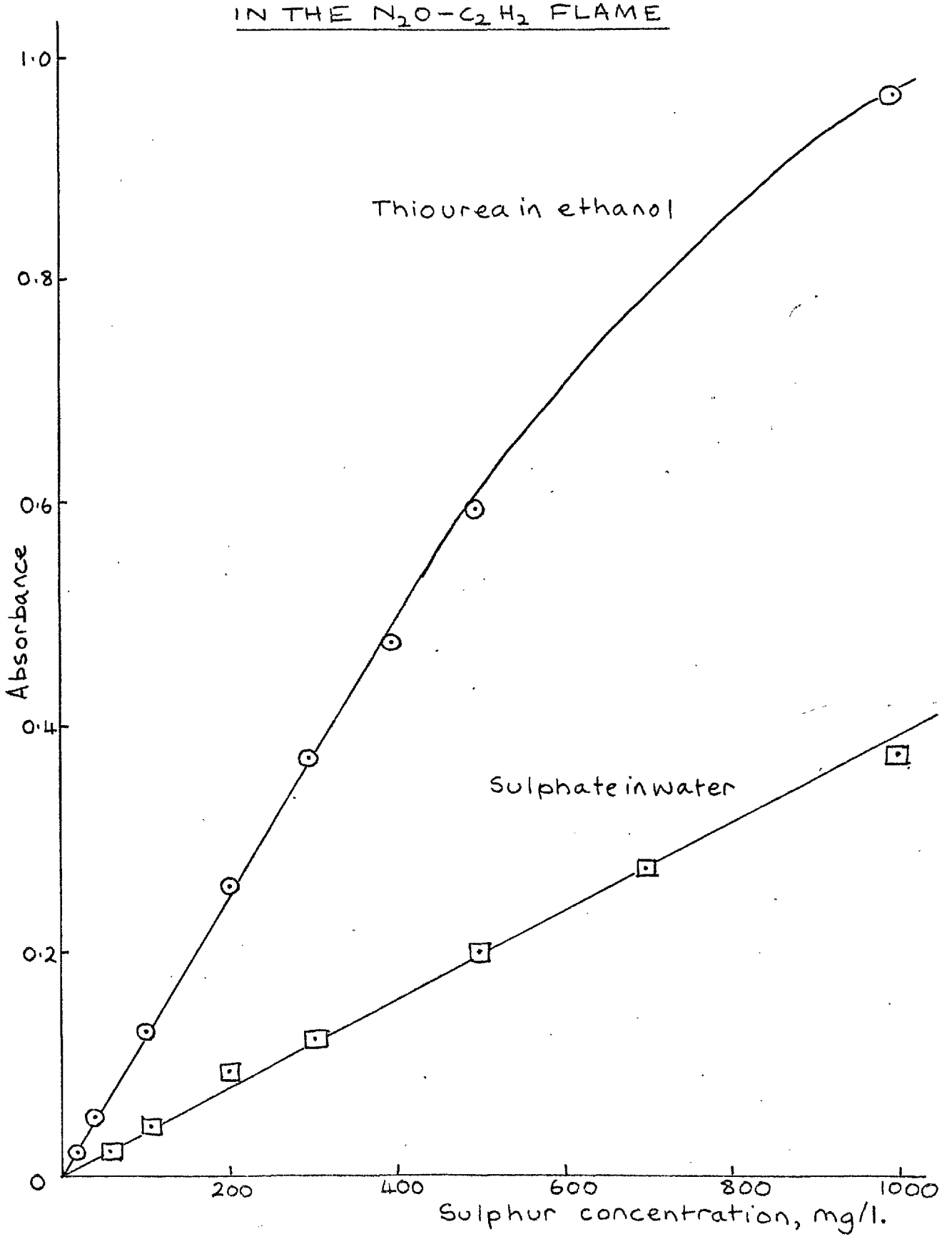

FIGURE 16 ABSORPTION PRODUCED BY 1000 MG/L SULPHUR INTRODUCED INTO THE SEPARATED $N_2O-C_2H_2$ FLAME IN DIFFERENT FORMS

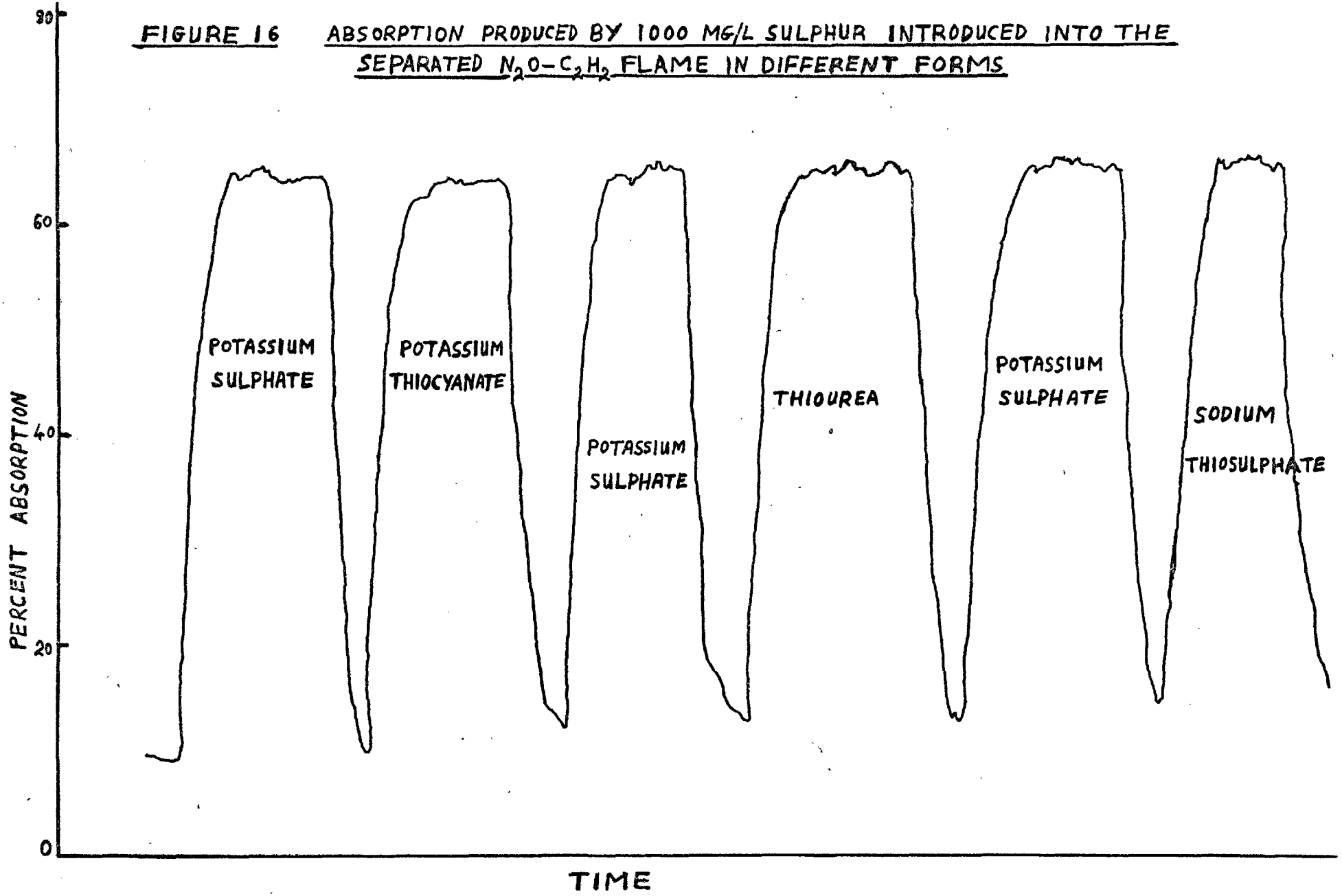

observed on introduction of the sulphur as thiourea in ethanol is fully accounted for by the improved nebuliser efficiency with the organic solvent.

2.9 The suitability of methyl iso-butyl ketone as a solvent for atomic absorption spectroscopy of sulphur

It was found that nebulising methyl iso-butyl ketone (MIBK) directly into a separated flame adjusted for aqueous solution caused the flame to become ultra-rich and lift off. A stable flame could be obtained by first nebulising the organic solvent into the unseparated flame, reducing the acetylene flow to compensate for the additional fuel supplied by the ketone, and then separating the flame. An acetylene flow rate of approximately 3.0 l/min was found satisfactory, compared to the 4.2 l/min used previously. The high flame transparency (64% of that of nitrogen) demonstrated previously at the 180.7 nm line at the optimum fuel flow rate for the determination of sulphur in aqueous or ethanolic medium was also achieved when MIBK was nebulised.

2.10 Response to different sulphur compounds in MIBK

When standard solutions of various sulphur compounds in MIBK were nebulised into the flame, higher absorbances were obtained than for the same sulphur concentration in aqueous solution. This would be expected because of the enhanced nebuliser efficiency when aspirating MIBK, compared to water. However, it was also found that different responses were obtained from the same sulphur concentration in MIBK when the sulphur was present in different compounds. This appeared to be linked with the volatility of the solute; Table 4 compares the absorption sensitivities and vapour pressures for various compounds.

It seems that extensive vaporisation of volatile compounds takes place in the expansion chamber of the indirect nebuliser, resulting in an anomalously high proportion of the solute being transported into the flame, and consequently giving a higher

Table 4

Variation of AAS sensitivity with vapour pressure for sulphur compounds

Compound	Approx. vapour pressure (mm Hg at 25°C)	AAS sensitivity for sulphur (mg/l / 1% absorption)
Dibenzyldisulphide	negligible	2.7
t-Butyldisulphide	0.5	2.7
t-Butylsulphide	5	2.0
Thiophen	80	0.6

absorption sensitivity.

A similar effect has been observed by Kirkbright, West and Wilson (40) in the determination of volatile organic compounds of iodine by atomic absorption spectrometry, and the same effect has also been reported for the determination of organo-lead compounds in petroleum.

It would appear from the results in Table 4 that either dibenzyldisulphide or t-butyldisulphide might be employed as a standard for the determination of sulphur in involatile materials. Dibenzyldisulphide does, however, have an advantage as a standard compound, since it is readily available as a pure crystalline solid and can therefore be conveniently weighed out for making standard solutions. It was, in fact, recommended as a standard for micro-analysis because of its desirable properties, which accounts for its ready availability in the pure state.

2.11 Determination of sulphur in oil

Most crude mineral oils contain appreciable amounts of sulphur; many refined petroleum products also contain significant amounts of this element. As a result of the toxic and corrosive effects of the sulphur dioxide produced when these materials are used as fuels and lubricants, the determination, and subsequently control, of the sulphur content of crude oils

and refined products is of great importance. A number of sensitive, precise and accurate methods for the determination of total sulphur in oils are applied routinely. These usually depend on prior combustion of the oil (by the Wickfold method) followed by volumetric or gravimetric determination of the sulphur dioxide evolved as sulphate (41). A variety of instrumental techniques, such as molecular absorption spectrophotometry (42), conductimetric and high frequency titration, radiometry(43), and microcoulometry (44) have been proposed to replace the simple volumetric or gravimetric determination of the sulphur dioxide recovered after combustion. Although these methods are sensitive, the combustion process may be time consuming and their reliable routine application requires considerable operator skill. The direct determination of total sulphur in oils without recourse to sample combustion has been successfully undertaken by X-ray fluorescence spectroscopy (45, 46) and by neutron activation analysis (47).

It is possible, in view of the fact that no great sensitivity is required, that the atomic absorption method might be applicable to the determination of sulphur in oil.

Procedure

A sample of the oil (about 1 g) was weighed and dissolved in 100 ml MIBK. This solution was nebulised into the separated nitrous oxide-acetylene flame, and the absorption at 180.7 nm measured. The concentration of sulphur was calculated by reference to a calibration curve prepared with standard solutions of dibenzyldisulphide in MIBK. The calibration curves were linear up to 400 mg/l.

Results

Table 5 gives some results obtained by the above technique.

These results suggested that the basic atomic absorption technique could be applied to the particular problem, but that the instrumental assembly was inadequate for the task at its present stage of development.

Table 5

Results obtained for determination of sulphur in oils

Sample no.	Sulphur content % w/w		%Error relative to standard method
	Mean for AAS and standard deviation	Standard method	
13 Crude oil L	1.53 ± 0.16	1.36	+ 12.5
14 Crude oil H	1.65 ± 0.02	1.60	+ 3.1
15 Crude oil K	2.74 ± 0.21	2.50	+ 9.6
1 Leaded gear oil	0.51 ± 0.04	0.49	+ 4.1
2 Fuel oil	2.1 ± 0.15	1.97	+ 6.6

CHAPTER 3

SOME IMPROVEMENTS TO THE INSTRUMENTAL SYSTEM

3.1 Limitations of the original instrumental system

The performance of the instrumental system described previously was not entirely satisfactory. Difficulties centred largely on a lack of stability, both in the spectral source's output and also in the RCA microammeter which was used to amplify the signals from the photomultiplier before they were displayed on the potentiometric chart recorder. Another important source of noise arose from turbulance in the various gases supplied to the flame. This led to variations in the flame transparency, giving rise to low frequency 'flicker' noise on the output signal. There was also a great deal of high froquency noise associated with the signal.

The various noise factors necessitated the use of very long damping time constants on the recorder; for much of the work a 1000 μF capacitor in parallel with a 20 Kohm resistance was employed on the recorder input. This gave the system a response time of approximately 100 seconds for full scale deflection.

However the use of long time constants merely reduced the the effect of high frequency noise; it had no effect on the low frequency noise and drift. Such a result was not unexpected, and therefore other possible readout systems were investigated.

3.2 Discussion of ac modulated detection systems

AC amplifiers are generally much more stable than dc amplifiers of equivalent gain and sensitivity. Moreover the use of an ac detection system may allow exploitation of the technique of selective signal modulation combined with phase sensitive detection. This technique is widely advertised as providing substantially improved (i.e., smaller) noise-equivalent bandwidths (48). The basic principle of the system is that the desired signal is modulated at a known frequency by a reference

signal; the signal then undergoes some process of interest whose effect is to alter the signal amplitude. The modified signal is then fed to an amplifier which may be either tuned to the reference signal frequency or wideband. This amplifier selects from the combined signal and noise those components within its bandwidth, amplifies them, and then passes the amplified signal to a phase-sensitive detector. This device is modulated by the reference signal so that components of the input which are in phase with the reference are detected, whilst out of phase components are rejected. Such systems, often known as "lock-in" amplifiers, can extract minute signals of a specific waveform and frequency from a background of overwhelming noise.

Lock-in amplifiers are widely used in atomic absorption, where their noise-rejection capabilities are exploited to reduce the effect of flame background emission. Careful selection of the signal modulation frequency to coincide with a minimum in the noise spectrum of the flame aids this process considerably (49). Modulation of the spectral source output may be achieved either by mechanical chopping of the light beam, or by variation of the electrical power supplied to the source.

Several workers have reported the successful operation of electronically modulated electrodeless discharge lamps (50); they noted that at the modulation frequencies employed, up to 100 KHz in one case (51), it was not possible to obtain a 100% depth of modulation, i.e., the output always contained a dc component.

This means that the modulation process reduces the effective signal power compared to the equivalent dc situation.

3.3 Tests on some practical ac systems

Experiments were made using the lock-in amplifier from a Techtron AA4 spectrometer (Techtron Pty., Melbourne, Australia) to detect the photomultiplier output; the resultant signal was then displayed either on its meter or at a potentiometric recorder. The electrodeless discharge lamp spectral source was modulated electronically at 285 Hz, and the gating circuit of the amplifier synchronised with the source modulation.

Experience showed that the performance of this new arrangement was much inferior to that of the original dc instrumentation. The noise was relatively much greater, and the absolute size of the signal much smaller (about 4 mV compared to 400 mV), so that the overall signal-to-noise ratio was appreciably degraded.

A much more sophisticated readout system was also tested, incorporating an AIM system 5 lock-in amplifier (AIM Electronics Ltd, St. Ives, Huntingdon). A block diagram of the instrumental system is given in Figure 17. In this case both electronic modulation of the electrodeless discharge lamp and mechanical chopping of the light beam were tested as methods of signal modulation. The stability of this amplifier system was very much better than that of the RCA microammeter, and it was not possible to observe any drift in the zero level, which had characterised the previous readout assembly. However the overall signal-to-noise ratio of the system was still inferior to that of the initial apparatus.

Brief tests with a Brookdeal 401 lock-in amplifier (Brookdeal Electronics Ltd, Bracknell, Berks) yielded similarly disappointing results.

3.4 Some further investigations into the nature of the signal

The output signal from the photomultiplier was amplified by a wide-band amplifier (AIM model ACA 123, bandwidth 4MHz - -3dB), and examined with a Tecktronix 551 four channel oscilloscope (bandwidth 60 MHz - -3dB).

Comparison of the reference waveform and the photomultiplier output revealed that the latter bore little resemblance to the former. It was found that the photomultiplier output consisted not of a small continuous alternating current but rather of a series of randomly spaced discrete pulses. Each pulse was of considerable amplitude, and had a rise time which exceeded the bandwidth of the amplifier.

Consideration of the problem elucidated a number of facts, which when taken together seem to account satisfactorily for the above results:

1. Light is received by a photomultiplier as discrete

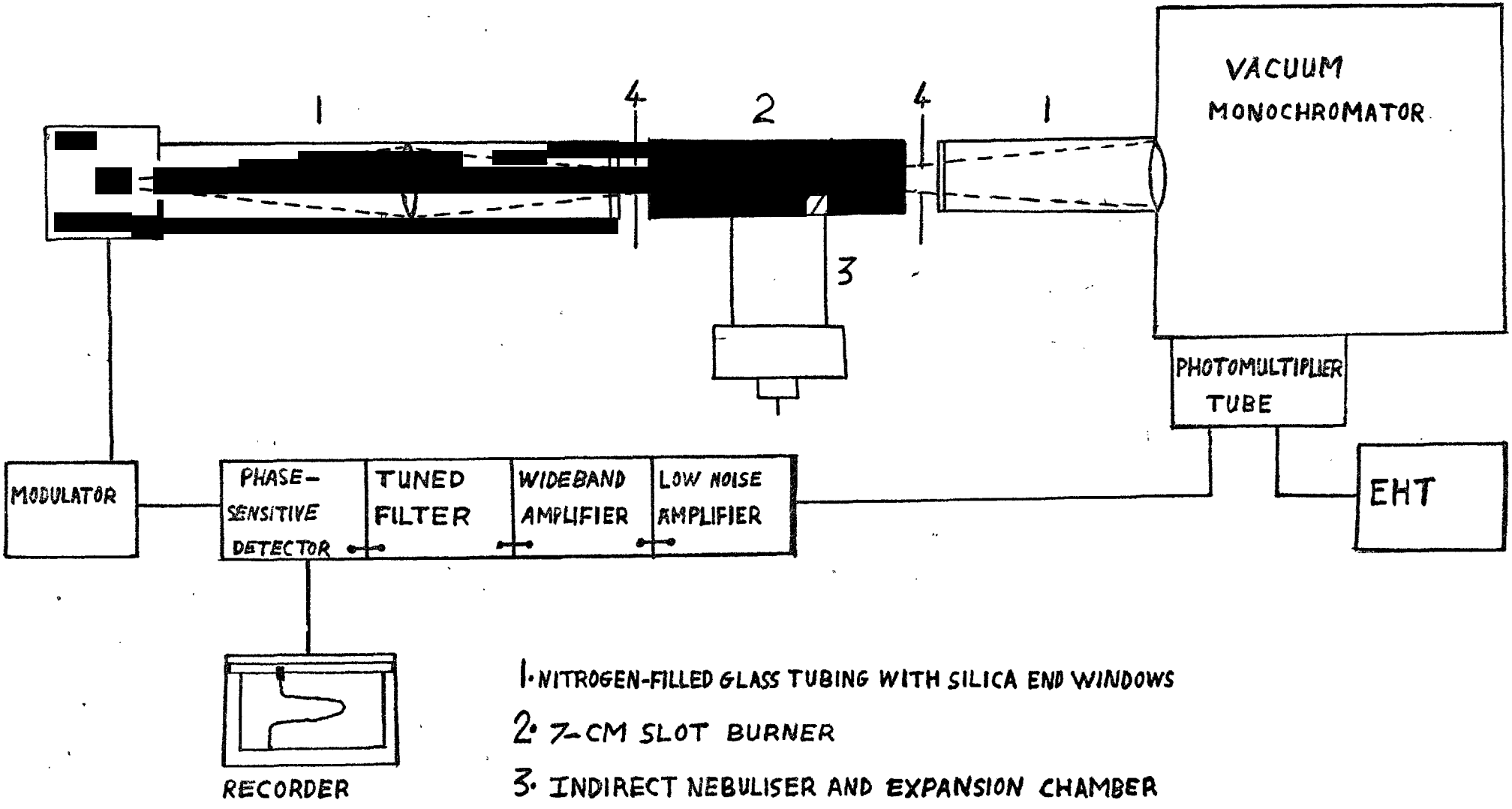

1. NITROGEN-FILLED GLASS TUBING WITH SILICA END WINDOWS
2. 7-CM SLOT BURNER
3. INDIRECT NEBULISER AND EXPANSION CHAMBER
4. COLLIMATING SLOTS

FIGURE 17

INSTRUMENTAL ASSEMBLY USING A LOCK-IN AMPLIFIER

particles i.e. photons. After allowing for the quantum effiency of the photocathode, each photon causes the photomultiplier to emit a pulse of electrons, which, in the absence of external damping, has a rise time of a few nanoseconds, and a considerable peak height.

2. At high light levels the pulses from the photomultiplier are emitted so frequently that they become indistinguishable from one another, and a pseudo-continuous output current is obtained.

3. The point at which the electrical signal appears as a pseudo-continuous current rather than discrete pulses depends (for a given amplifier bandwidth) on the frequency of occurrence of pulses and not on their amplitude. Thus it depends on the light intensity, and not on the current generated by the photomultiplier. This point touches on an important misconception, created by the popularity, among commercial instrument manufacturers, of inexpensive photomultipliers with inherently low gains. If such a photomultiplier is employed for photometry, quite high light fluxes will produce minute currents, which will however still have a pseudo-continuous nature because of the large number of photons involved. In these cases sophisticated amplifiers may well provide an enhanced signal-to-noise ratio (although similar results might be obtained more cheaply with a better photomultiplier).

However if a very high gain photomultiplier, such as the EMI 6256 B employed here, is considered, a fairly large current (total charge per unit time) will be generated from a small number of photons. In these experiments, equivalent dc currents of about 20 nanoamps were obtained with photomultiplier output rates of about 1000 pulses per second. At such very low light levels the "shot" noise observed with analogue measurement techniques will be very large; the only effect of modulating the system and using a lock-in amplifier is to further reduce the total number of photons received by the detector and so increase the shot noise.

3.5 Discussion of phase sensitive detection and selective modulation

This then is the fundamental fallacy in the widespread claims that lock-in amplifiers, combined with modulated sources, are the ultimate answer to measurement problems in low level photometry. The proponents of phase sensitive detection fail to take into account the particulate nature of light.

The advantage of such selective modulation techniques in flame spectrophotometry would therefore appear to reside not in their ability to process ultra low level signals, but in their ability, at higher light levels, to satisfactorily discriminate between a modulated signal and an unmodulated, unwanted background.

In this study of atomic absorption spectrophotometry in the vacuum ultra-violet, it has been demonstrated that no background emission from the flame can be detected, but that very low light levels are being measured. The use of lock-in amplifiers and selective modulation is of no value in such circumstances. Any measurement technique which is to be useful in these circumstances must utilise the entire available signal in order to avoid degrading the signal-to-noise ratio unnecessarily.

3.6 Photon counting techniques

This subject has recently been reviewed by Malmstadt et al. (52) and also by Sharp (53).

Photons striking the cathode of the photomultiplier cause the tube to emit pulses. The number of pulses produced is proportional to the light intensity. The basis of the photon counting technique is to record the number of pulses from the photomultiplier using a digital counter. This has several advantages, some concerned with the better technical characteristics of digital electronics which may be employed, and some with the physical properties involved.

Successful operation of photon counting systems requires that the instrumental assembly fulfil a number of criteria, which have been theoretically evaluated by Sharp (53). The most important practical points are:

1. The photomultiplier-counter interface should possess a minimum of stray capacitance (which degrades the pulse shape, reduces the pulse peak height and leads to counting losses).

2. The counting system must have the ability to separate closely spaced pulses, otherwise counts will be lost due to pulse pile-up. It has been shown (53) that if count losses due to pulse pile-up are to be kept below 1% of the total count, then the count rate must be less than 0.01 divided by the counter dead time. Where a digital frequency meter is employed as a counter the parameter specified is usually the frequency bandwidth (F) for the -3dB point. In this case the maximum count rate for 1% loss is approximately 0.03F.

3. The photomultiplier employed should have low dark current, good stability, the highest possible gain and should also produce sharply defined, narrow, output pulses.

In practice these conditions are not difficult to meet, high speed counters and suitable photomultipliers being commercially available.

A schematic diagram of the instrumentation employed for low level spectrophotometry by means of photon counting is given in Figure 18.

One immediate improvement due to the use of photon counting techniques is the virtual elimination of amplifier drift; the main sources of drift in this detection system are:

1. Variation in the EHT voltage causing variations in the photomultiplier gain and hence in the pulse height spectrum, which alters the number of pulses crossing the counter threshold.

2. Variation in the threshold level of the counter.

3. Drift in the photomultiplier tube gain.

In practical systems these factors can be held to exceedingly low values (typically EHT noise can be only a few parts per million), so that the detection system is essentially drift free.

Another, theoretical, advantage of photon counting is that it is an integral technique. The merits of signal integration

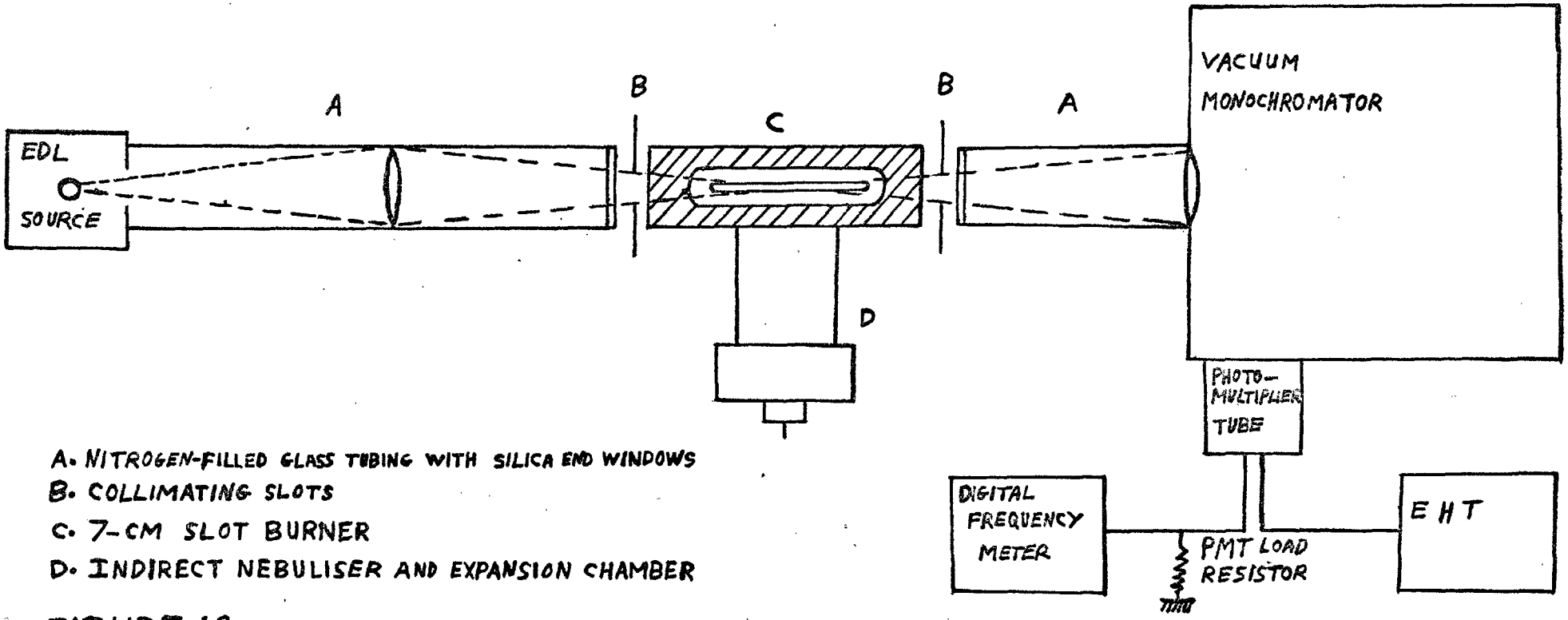

A. NITROGEN-FILLED GLASS TUBING WITH SILICA END WINDOWS
B. COLLIMATING SLOTS
C. 7-CM SLOT BURNER
D. INDIRECT NEBULISER AND EXPANSION CHAMBER

FIGURE 18

INSTRUMENTAL ASSEMBLY USING PHOTON COUNTING

have been fully discussed by L'vov (10). The sensitivity of an integration technique is a function of the integration time; digital integration of photon counts is advantageous compared to dc-capacitive integration because the drift free nature of the technique makes long integration periods possible. This provides better signal-to-noise ratios, and makes possible the detection of exceedingly low light levels.

Some reduction can also be made in the effective dark current, though this is a subject which must be treated with caution, as rather exaggerated claims have been made on occasion. Electron pulses due to photons striking the cathode surface of the photomultiplier form a characteristic distribution of pulse height versus number (54). These characteristics may be exploited, by means of pulse height discrimination, to reject some of the dark current and its associated noise.

Dark current pulses arise from a number of processes within the photomultiplier, including:

1. Thermionic emission from the photocathode. Since these pulses are produced by electrons emitted by the cathode, they undergo the full amplification due to the photomultiplier tube, and have similar distribution of pulse height to that of photon induced pulses. It is not therefore possible to discriminate against thesepulses.
2. Emission from the secondary electrodes of the photomultiplier. Such pulses do not receive the full amplification of all the stages of the dynode chain, and hence are generally smaller than cathodic pulses. They can be partially rejected by means of pulse height discrimination.
3. Radio-active processes. Pulses may originate from cosmic rays, background terrestrial radiation, and radioactive isotopes present in the material of construction of the photomultiplier . The principle problem occurs when glass envelopes are used for the tubes; the unstable potassium isotope ^{40}K may then contribute appreciably to the dark current of the photomultiplier. Use of quartz envelopes, and careful selection of other constructional materials obviates this difficulty.
4. Ionisation of residual gas inside the photomultiplier

tube. The contribution made to the dark current by ionisation of residual gases in the tube is uncertain. Theoretically pulses due to gas ionisation could have a mean pulse height greater than that of photon pulses, and might be susceptible to pulse height discrimination, which would therefore result in improved signal-to-noise ratios. No convincing experimental demonstration of this possibility has been given.

A contribution to the effective dark current is also made by externally generated electrical interference. This arises from a whole host of specific causes but may be divided into two general classes, mains-borne interference and radiative interference. Mains-borne interference is generated by such articles as inadequately suppressed electric motors, and the switching on or off of heavy electrical loads. Radiative interference may arise from, for example, electrical discharges (e.g. lightning), motor car ignition systems, electric motors, radio transmitters and faulty electrical switchgear. Electrical interference is most effectively treated at its source; however mains-borne interference can be considerably reduced or even eliminated by suitable filters placed in the mains supply line.

The electrical environment of the equipment has considerable bearing on the previous discussion on the reduction of effective dark current by means of pulse height discrimination, since the use of very low threshold levels for pulse counting makes the system very susceptible to external electrical interference. The amount of electrical interference encountered will therefore set a minimum value for the trigger level of the counter, and this may be more important in practice than the pulse height distribution of dark current pulses originating from the photomultiplier.

The general conclusion to be drawn from this discussion is that use of a minimum threshold level below which pulses are ignored is advantageous, but that more sophisticated techniques of pulse height discrimination, such as the use of upper thresholds and voltage windows are unnecessary. It has been claimed (55) that effects due to pulse height overlap can be eliminated by pulse height discrimination, leading to an extended linear

counting range. However pulse overlap is only significant at very high count rates (i.e. high radiation intensities) and in such circumstances the problem can be more simply resolved by use of an analogue detection system.

It is of interest to note that the theoretical error curve calculated for precision absorption measurements is different for photon counting and analogue readouts (52). If the reference and sample counts are N_r, N_s, with standard deviations σ_r, σ_s respectively, then the percentage relative standard deviation, E_A, of the absorbance measurement is given by

$$E_A = 0.434 \left(\frac{\sigma_r^2}{N_r^2} + \frac{\sigma_s^2}{N_s^2} \right)^{1/2} \cdot \frac{100}{\text{absorbance}} \qquad 3.1$$

Theoretically the photon counts should follow a Poisson distribution (52) so that the standard deviation of a particular measurement should equal the square root of the count. Table 6 gives results of calculated errors for absorbance measurements at typical count rates, assuming Poisson statistics, and Figure 19 displays the information graphically, together with the calculated error curve for an analogue readout based on a 1% scale reading error.

It can be seen that the presentation of the information in digital form improves the precision of absorbance measurements. Practical digital counters have a reading error of $\pm$ 1 in the least significant digit displayed, but this does not affect the general conclusion.

A final advantage which may be cited for photon counting techniques is that the equipment used can be readily interfaced with data processing equipment, permitting more sophisticated statistical treatment of results. It is equally pertinent to comment that the vast quantities of numerical data produced by photon counting force the analytical chemist to engage in a great deal more arithmetical calculation than would normally be required. It would be unwise to apply photon counting techniques to routine analytical work without making proper provision for automatic data processing.

Table 6

Theoretical error in absorbance at different count rates

Reference counts = 1×10^5

Sample counts	Absorbance	Theoretical percentage error
9.9×10^4	0.0044	44.5
9.8×10^4	0.0088	22.0
9.7×10^4	0.0132	14.8
9.5×10^4	0.0223	8.80
9.0×10^4	0.0458	4.35
8.0×10^4	0.0969	2.12
7.0×10^4	0.1549	1.35
6.0×10^4	0.2218	1.01
5.0×10^4	0.3010	0.790
4.0×10^4	0.3979	0.645
3.0×10^4	0.5229	0.546
2.0×10^4	0.6989	0.480
1.0×10^4	1.0000	0.461
5.0×10^3	1.3010	0.428
3.0×10^3	1.5229	0.528
1.0×10^3	2.0000	0.690
5.0×10^2	2.3010	0.845
1.0×10^2	3.0000	1.46

FIGURE 19 PRECISION AS A FUNCTION OF ABSORBANCE

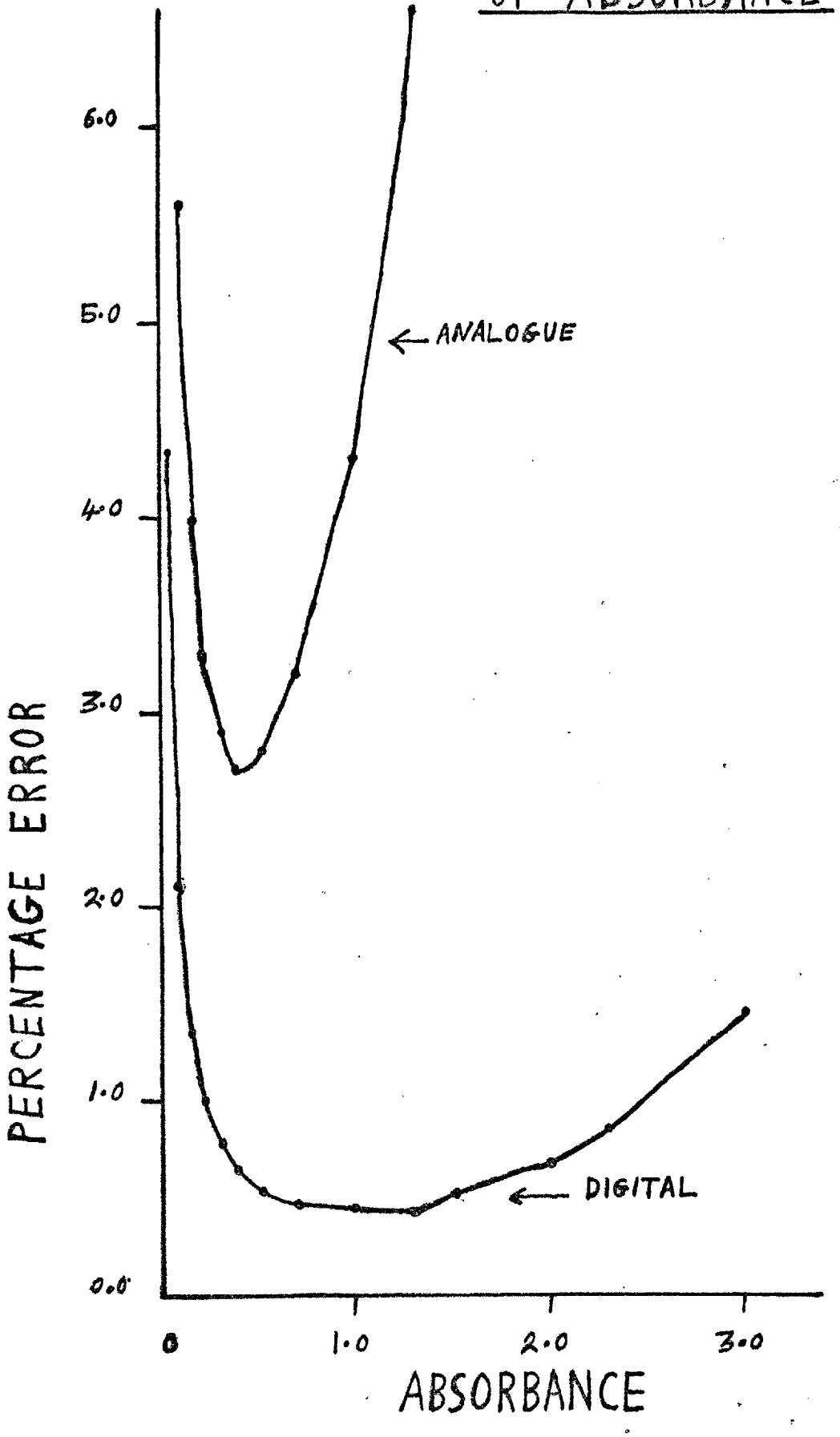

3.7 A practical photon counting system

Initial tests, feeding the photomultiplier output to a 1 Kohm load resistor across the input of a digital frequency meter (TSSA6636/3M, Venner electronics, New Malden, U.K.)which recorded the number of pulses received, suggested that the photon counting technique merited more detailed investigation. Certain practical problems were resolved by slight modifications to the instrument. For instance, the Hilger and Watts photomultiplier power supply previously employed was replaced by a Brandenburg 472R EHT unit (Brandenburg Ltd., Thornton Heath, U.K.), which eliminated spurious pulses due to the EHT unit. This necessitated rewiring the resistor chain on the photomultiplier (see Figure 20) to provide a potential on the last dynode. Another modification was to reroute the signal cable from the photomultiplier to reduce its length, minimising the stray capacitance of the cable, and so maximising the frequency bandwidth of the system and ensuring the maximum pulse height (53). This was accomplished by placing the digital frequency meter on a shelf built onto the monochromator, and connecting its input to the photomultiplier anode by a short length of co-axial cable (c. 8 inches)routed through a hole drilled in the monochromator case.

Mains-borne interference was reduced by the insertion of an RF mains filter (Model L1829, Belling and Lee Ltd., Enfield, U.K.) in the power supply line.

Various combinations of photomultiplier voltage and load resistance were tried, and it was found that when the frequency meter's trigger level was set at 10 mV an EHT voltage of 1620 V, combined with a load of 470 ohms, was satisfactory.

In order to calculate the absorbance due to a particular solution, it was necessary to measure the incident intensity, i.e. number of counts, at 100% transmission (N_T), zero transmission (N_B), and while nebulising sample (N_S). Values for N_T, N_B, and N_S were obtained by taking the total of ten ten-second counts for each.

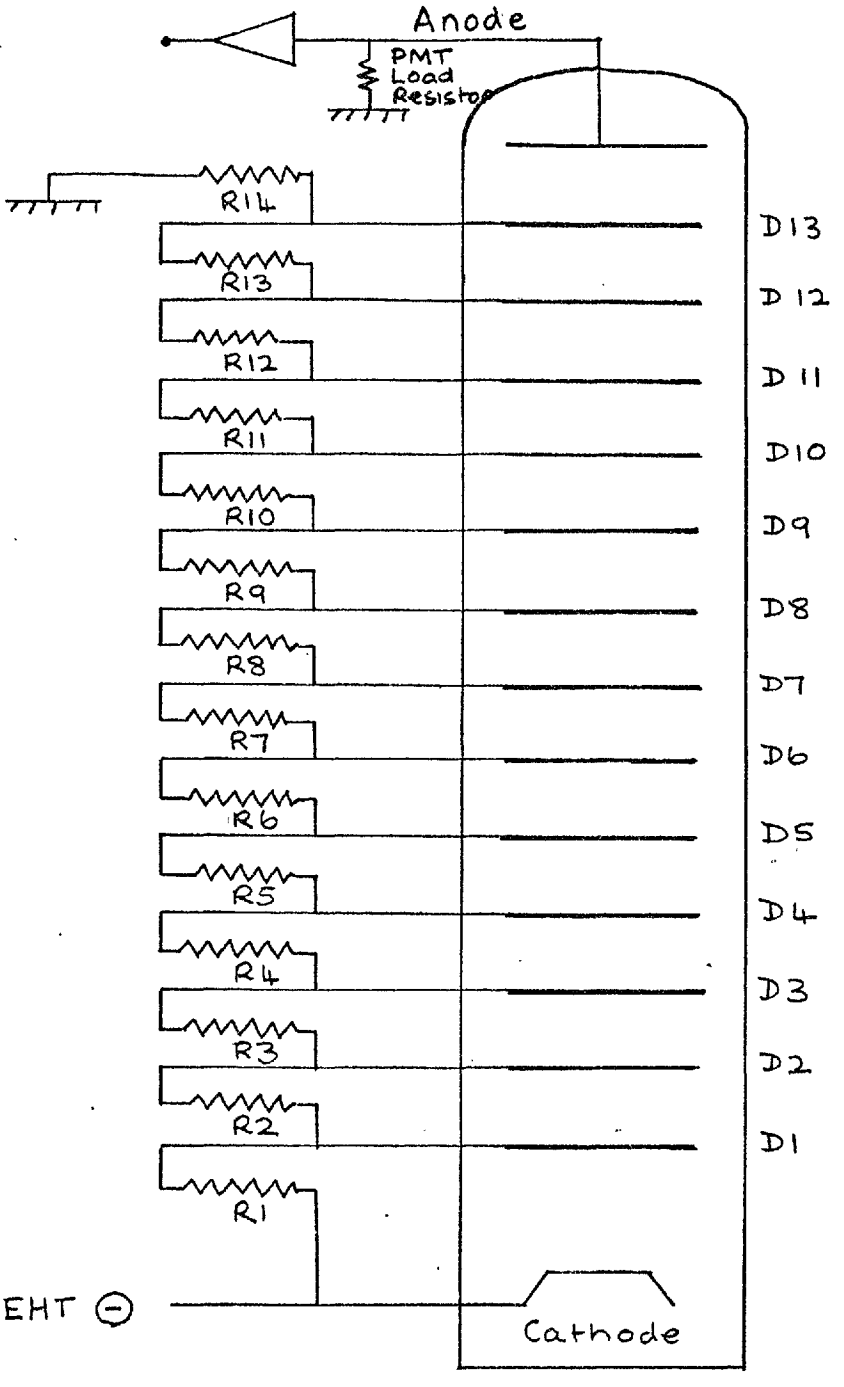

R1 – R14 = 250 Kohm, 1/4w (1%)

FIGURE 20

MODIFIED PHOTOMULTIPLIER DYNODE RESISTOR CHAIN

3.8 Application of the improved instrumental system to the determination of sulphur in oil

The new instrumental system was tested by determining the sulphur contents of various oil samples, some of which had previously been examined with the original instrument, so facilitating comparisons between the two.

Sample preparation

1. Dilution procedure:

0.2 to 1.0 g samples of oil were weighed using a short length of clean glass tubing as a disposable pipette. Each oil sample was then dissolved in methyl iso-butyl ketone, and diluted to volume in a 100 ml flask. The weight of oil taken was chosen on the basis of two criteria:

(a) The anticipated sulphur content of the final solution should fall in the convenient working range 40 - 400 mg/l, as the calibration curve was known to be linear up to 400 mg/l.

(b) The nebulisation characteristics of the oil sample solution should not differ significantly from those of the standard solutions due to different viscosity, density or surface tension. Difficulties of this type should not be experienced with solutions containing less than about 0.5% w/v of oil, but this point can readily be checked by comparing the sample uptake rate and nebuliser efficiency for both samples and standards.

Each oil solution was nebulised into the separated nitrous oxide-acetylene flame, and its absorbance measured at 180.7 nm.

It was found more convenient to repeatedly spray a single standard in the middle of the working range, and compare the mean absorbance with the sample solution's absorbance, rather than to construct a separate calibration curve for each experiment. This approach facilitated calculation of the final result from the digital information provided by the frequency meter. The mean value of six readings was taken for each solution.

2. Standard additions procedure:

A weighed quantity of oil, chosen to give a final concentration, after dilution, in the working range 40 - 400 mg/l was made up to volume in a 50 ml flask with methyl iso-butyl

ketone. Two 20 ml aliquots of the solution were then transferred to 100 ml flasks. To the second of these a standard addition equivalent to 50 mg/l of sulphur was made and the solutions were diluted to volume with methyl iso-butyl ketone. The solutions were then nebulised into the separated nitrous oxide-acetylene flame and the concentration of sulphur in the sample solution calculated from the ratio of their absorbances at 180.7 nm.

Selection of the standard compound

In accordance with the previous findings, dibenzyldisulphide was employed as the standard compound for oil analysis. Difficulties were not expected due to the enhanced 1% absorption sensitivities obtained at 180.7 nm with volatile sulphur compounds, as in refined oil products the sulphur compounds of high volatility are largely removed in processing. For crude oils the presence of hydrogen sulphide and high volatility sulphur compounds might be expected to lead to high results when a non-volatile sulphur compound is employed as standard; as described below, however, this effect was not observed. Presumably the volatile sulphur components in crude oil are lost before analysis.

Results and discussion

The results obtained for the determination of sulphur in oils by both the dilution procedure and the standard additions procedure are shown in Table 7. Each of the values in column 3 represents an oil sample taken through the sample dilution and recommended procedure. The absorbance for each of these diluted samples was measured six times and the mean value used to calculate the sulphur content. The three values shown for each oil were obtained in different experiments conducted on different days over a period of several weeks; the standard deviations shown in column 4 therefore also take into account the long term repeatability.

The values obtained by atomic absorption spectrometry for the oil samples, whose sulphur contents were determined by reference to a pure standard solution of dibenzyldisulphide in methyl iso-butyl ketone, show a small systematic error compared

Table 7 Results obtained for determination of sulphur in oils

SAMPLE NO.	SULPHUR CONTENT, % w/w				
	Combustion Method (41)	X-ray Method (46)	AAS determination This work.	Mean for AAS and standard deviation	% Error relative to standard method
1. Leaded Gear Oil	0.49		0.50, 0.46, 0.52	0.50 ± 0.02	+ 2.0
2. Fuel Oil	1.97		1.96, 1.92, 2.01	1.96 ± 0.06	- 0.5
3. Fuel Oil	2.65		2.65, 2.67, 2.71	2.68 ± 0.03	+ 1.1
4. Light Crude		1.44, 1.47 > 1.45	1.25, 1.31, 1.26	1.27 ± 0.12	- 12.4
5. Heavy Crude		1.75, 1.74 > 1.74	1.50, 1.59, 1.60	1.56 ± 0.05	- 10.3
6. Crude		2.68, 2.70 > 2.69	2.55, 2.41, 2.51	2.49 ± 0.06	- 7.4
7. Fuel Oil A		2.64, 2.69 > 2.66	2.46, 2.59, 2.44	2.50 ± 0.07	- 6.0
8. Fuel Oil B		2.69, 2.77 > 2.73	2.43, 2.37, 2.25	2.35 ± 0.07	- 13.9
9. Fuel Oil C		2.87, 2.97 > 2.92	2.52, 2.44, 2.85	2.60 ± 0.18	- 11.0
10. Fuel Oil D		1.63, 1.67 > 1.65	1.56, 1.48, 1.44	1.49 ± 0.10	- 9.7
11. Crude A		0.109, 0.107 > 0.108		0.106±0.11†	- 1.9
12. Crude B		0.161, 0.155 > 0.158		0.159±0.009†	+ 0.6

† Standard additions method

to the mean values obtained by X-ray fluorescence. This most probably results from a slight mismatch in the viscosity characteristics between the diluted samples and standard solutions. This could possibly be eliminated if a sulphur-free base oil of similar viscosity was available to add to the standard solutions to match the nebulisation characteristics. Even without matching the sample and standard solution viscosities closely, however, the accuracy attained compares quite favourably with the spread of results obtained between laboratories for sulphur determination in similar oils using the X-ray fluorescence spectrometry method recommended by the American Society for Testing and Materials (45). No significant systematic error was observed in the values for sulphur content obtained for the oils treated by the standard additions technique. This confirms that a mismatch between sample and standard viscosity characteristics is responsible for the error in the conventional technique; when suitable sulphur-free base oils are not available, therefore, use of the standard additions technique is preferable, particularly for examination of samples of low sulphur content (less than 0.5%) where the smaller dilution factor required would result in more severe mismatch.

The results confirm that the direct nebulisation of diluted oil samples into the separated nitrous oxide-acetylene flame permits the direct determination of their sulphur content by atomic absorption spectrometry at 180.7 nm with acceptable accuracy and precision. The attainable sensitivity should be sufficient for the determination of sulphur in most refined oils, with the exception of motor spirit.

3.9 Conclusions

Comparison of the results obtained with the various detection systems tested shows that the photon counting technique performed better than the dc or ac systems, more precise measurements being obtained in a shorter time.

Practical problems of susceptibility to external electrical interference, which are totally ignored in the literature, can be satisfactorily overcome by careful design. This problem is

of greater significance in maximising the signal-to-noise ratio of photon counting than the frequently discussed techniques of pulse height analysis and pulse height discrimination, and merits more intensive study.

It is suggested that full exploitation of the potentialities of the photon counting technique can only be achieved by integrated design of the monochromator and counting detection system so as to achieve the widest linear counting range and provide maximum possible screening from external noise sources. In any practical design of photon counter, provision should be made to reduce the arithmetical calculation required either by employment of ratemeter attachments interfaced with a potentiometric chart recorder (56) or by provision of computing systems.

Further improvements in the detection limit for sulphur would be obtained if the spectral source were less unstable. Additionally, it would be desirable to obtain spectral lines which were sharper and more intense. One possible method of improving the performance of the electrodeless discharge lamps used in this study would be to fill them with gaseous sulphur compounds such as sulphur dioxide or hydrogen sulphide, rather than solid sulphur. Such a step would give much better control over the amount of sulphur introduced into the lamp, and should therefore facilitate the production of intense, sharp line sources.

Some preliminary experiments indicated that lamps filled with a mixture of 3 - 4 torr sulphur dioxide and an equal amount of argon emitted the sulphur 180.7 nm line, but no tests of the atomic absorption spectrometric characteristics of these lamps were undertaken.

A similar technique might also be used for phosphorus electrodeless discharge lamps, filling with phosphine, and likewise for arsenic and selenium.

CHAPTER 4

ATOMIC ABSORPTION SPECTROMETRY OF PHOSPHORUS

4.1 Introduction

The element phosphorus possesses a number of important resonance lines which might be suitable for atomic absorption spectrometry (32). Table 8 gives the relevant information, which is also shown graphically in the Grotrian diagram, Figure 21.

Sullivan and Walsh (57) reported the determination of phosphorus, using a hollow cathode atom cell, at the 177.5 nm line, but no further details of this work have appeared. Khartsyzov and L'vov (10, 18) successfully determined phosphorus using an electrically heated graphite cuvette, and stated that the highest absorption sensitivity was obtained at the 177.5 nm line. It is not clear, however, whether this study included the lower lying lines of the $3s^2 3p^3 - 3s\ 3p^4$ group. Manning and Slavin (58) observed absorption by phosphorus atoms in a flame; in this case the 213.547nm - 213.620 nm line pair, and the 214.911 nm line were used. These lines originate in excited state levels whose population is less than 1% of the total atomic population present; consequently a very poor absorption sensitivity would be expected. The observed values in a nitrous oxide-acetylene flame of 290 mg/l / 1% absorption for the 213.547 nm - 213.620 nm line pair and 540 mg/l / 1% absorption for the 214.911 nm line are therefore not surprising. These workers did however comment that a slightly better sensitivity would have been obtained had the monochromator employed been able to resolve the pair of lines at 213 nm. Manning and Slavin's results confirm the possibility of generating at least some phosphorus atoms in a flame.

It was therefore decided to investigate the atomic absorption characteristics of phosphorus, using a nitrogen separated nitrous oxide-acetylene flame as the atom reservoir. In view of the previous experience with sulphur, it was thought improbable that the CFAR unit of West and Williams (20) would provide sufficient energy for the efficient formation of phosphorus atoms.

Table 8

Some important resonance lines of the phosphorus atom (32)

Transition array	$3s^2 3p^3 - 3s3p^4$				$3p^3 - 3p^2(^3P)4s$		
Multiplet	$^4S^0 - {}^4P$				$^4S^0 - {}^4P$		
Wavelength (nm)	167.168	167.461	167.971		177.499	178.287	178.768
Lower energy level E_i cm^{-1}	0	0	0		0	0	0
Upper energy level E_k cm^{-1}	59820	59716	59535		56340	56090	55939
Statistical weight g_i	4	4	4		4	4	4
Statistical weight g_k	2	4	6		6	4	2
Oscillator strength f_{ik}	0.23	0.45	0.68		0.154	0.102	0.051
Uncertainty in f_{ik} value	>50%	>50%	>50%		≤25%	≤25%	≤25%
Transition probability A_{ki} (10^8 sec^{-1})	11	11	11		2.17	2.14	2.13

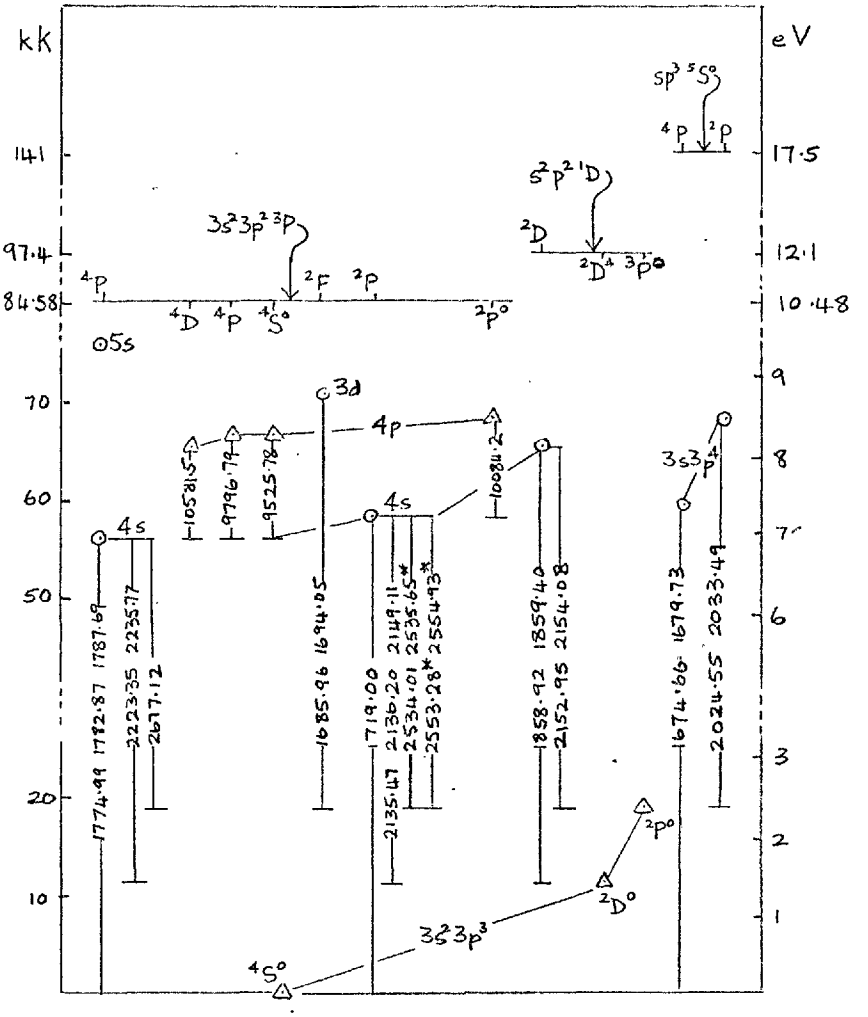

FIGURE 21

GROTRIAN DIAGRAM FOR PHOSPHORUS

The vacuum monochromator which was to be employed restricted the study to the 177.5 nm, 178.3 nm and 178.8 nm lines. It is not, in fact, clear whether any experimental study of the absorption characteristics of the shorter wavelength lines has ever been made; the values of oscillator strengths quoted in the literature (32) are the results of theoretical calculations. Certainly the values cited seem to indicate that the 167.971 nm line should yield the highest absorption sensitivity of any of the phosphorus resonance lines listed in Table 8.

4.2 Experimental

Apparatus

The shielded burner, optics and vacuum spectrometer employed previously (see Chapter 2) were used for this work. The photomultiplier used (Type 6256B, EMI Electronics Ltd., Ruislip, U.K.) was selected for lowest dark current, from a batch of ten. Photomultiplier high voltage was optimised for best signal to noise ratio.

A "photon counting" readout system was used, as before, except that a different digital frequency meter (TSSA 7737A, Venner Electronics Ltd., New Malden, U.K.) was employed. This frequency meter was provided with an adjustable pulse height trigger level which in this study was set at 60 millivolts to further discriminate against spurious pulses due to external interference.

Use of the profile control on the spectrometer enabled wavelength scanning over the narrow spectral range encompassing the three lines of interest.

Spectral source

Two types of spectral source were investigated:

1. A phosphorus hollow cathode lamp (S.J.Juniper & Co., Halstead, Essex, U.K.). This contained a hollow cathode made of indium phosphide contained in a nickel slug. The lamp was filled with neon. A hollow cathode lamp supply from a Techtron AA4 spectrometer (Techtron Pty., Melbourne, Australia) was used to provide the necessary electrical

power.

2. A microwave electrodeless discharge lamp (EDL). Blanks for the manufacture of EDL's were made from both "Vitreosil" and "Spectrosil" tubing (Thermal Syndicate, Wallsend, Northumberland, U.K.) of 8 mm bore, and were carefully outgassed before use by heating under vacuum. Various EDL's were prepared, loaded with red phosphorus, phosphorus pentoxide and triphenyl phosphine, and filled with argon. The microwave cavity employed for excitation of the EDL (Model 210L, Electro-Medical Supplies Ltd., Wantage, U.K.) was modified by the provision of watercooling pipes to remove excess heat.

Reagents

A stock solution containing 5000 mg/l of phosphorus was prepared by dissolving analytical reagent grade di-ammonium monohydrogen orthophosphate (5.3299 g) in distilled water (250 ml). Working standards were then prepared by dilution as required.

Stock solutions of the diverse ions used in the interference studies were also prepared from analytical reagent grade salts of the elements.

4.3 Spectral source characteristics

1. Phosphorus hollow cathode lamp

The hollow cathode lamp was found to be completely unsatisfactory for practical use. Some emission of the 213.6 nm, 214.9 nm and 253.6 nm lines was observed using the 1/2 metre Ebert monochromator from a Techtron AA4 spectrometer, but the intensity of the 177.5 nm line was so low as to be almost undetectable with the vacuum spectrometer. It was not therefore possible to make any atomic absorption measurements with the hollow cathode lamp.

2. Phosphorus electrodeless discharge lamp

Triphenyl phosphine was found to be unsuitable for manufacture of EDL's as it carbonised during the sealing off of the lamp and prevented a good vacuum seal being obtained.

EDL's were successfully prepared from both red phosphorus (reagent grade) and phosphorus pentoxide. Considerable difficulty was experienced in obtaining a satisfactory lamp. However the following conclusions were drawn:

(a) Lamps filled with red phosphorus were at least an order of magnitude more intense than those filled with phosphorus pentoxide.

(b) An argon filling pressure of ca. 3 torr was satisfactory.

(c) The minimum possible quantity of phosphorus should be used for filling EDL's. In this study the dose used was estimated as about 0.1 mg.

(d) It was considered immaterial whether Vitreosil or Spectrosil was employed for lamp manufacture, provided the blanks were properly outgassed, and the silica surface was free from blemishes.

(e) The lamps required very careful tuning using a reflected power meter.

If the phosphorus in the lamp was resublimed by heating in a flame, white phosphorus was obtained inside the lamp. After a microwave discharge had occurred in the EDL, the phosphorus changed to the red form.

Observation of the reflected power meter showed that the microwave excited discharge in the EDL took place in several stages, characterised by changes in both the reflected power and the optical emission. It is tempting to liken these steps with the various equilibria in the thermal dissociation of molecular phosphorus vapour (59), but this is a highly speculative suggestion.

The most successful method of initiating the lamps was found to be:

(a) Ignite at about 60 watts using a Tesla coil.

(b) Increase the applied power to maximum (200 watts) and adjust the cavity tuning stub until the reflected power drops to about 20 watts.

(c) Gradually reduce the applied power and retune the cavity after each step.

It appeared that the initially high power served to disrupt the phosphorus vapour into atoms which were then able to

take part in the plasma discharge at relatively low powers (about 60 watts was used).

The profile control of the vacuum spectrometer was used to scan over a narrow range ($\pm$ 1 nm approximately) of wavelengths centred on 178.2 nm. Only three spectral lines were observed within this range, with the relative positions appropriate to their identification as the 177.5 nm, 178.3 nm and 178.8 nm lines of phosphorus. No background emission from the lamp was detected; this may partly be a result of the very narrow (0.03 nm) spectral bandwidth of the monochromator.

A number of observations were made on the relative emission intensities of the three lines. These were carried out with the flame off, the optical system purged and nitrogen flowing through the burner shield. It was found that unpredictable changes occurred in the relative intensities of the lines. However the intensity ratios between the lines appeared to stabilise after the lamp had been running for several days. Final values of relative intensity observed were:

177.5 nm, 1.00: 178.3 nm, 5.61: 178.8 nm, 8.11.

The precise reason for the intensity ratios observed is not understood; theoretically the shortest wavelength line should be the most intense. One contributing factor may be light absorption by the residual oxygen in the optical path; apparently the 177.5 nm line coincides with a peak in the absorption spectrum of oxygen, whilst the other two lines lie in an adjacent trough (see Figure 1). Another point may be that the microwave plasma in the electrodeless discharge lamp is unlikely to be in thermal equilibrium, and this could invalidate the theoretical intensity predictions. A final, and important, consideration is the effect of self-absorption on the three lines. Since the 177.5 nm line theoretically has both the highest emission intensity and the highest absorption coefficient it will be the most strongly self-absorbed of the three lines, which would certainly influence the observed relative emission intensities.

4.4 Transmission characteristics of the nitrogen separated nitrous oxide-acetylene flame

It was found that the red feather zone of a fuel rich, separated, nitrous oxide-acetylene flame transmitted an appreciable proportion of each of the three phosphorus lines. As might be expected from the absorption spectrum of oxygen, the percentage transmission for the 178.8 nm line was greatest, and that for the 177.5 nm line least. Table 9 lists the maximum percentage flame transmission obtained at each line.

Table 9

Maximum flame transmission factors

Wavelength	Maximum percentage transmission
178.8 nm	63.80
178.3 nm	56.51
177.5 nm	27.78

The hundred percent transmission level was measured with the flame off, the optical path purged with nitrogen, and nitrogen flowing through the burner shield at the same rate as used for separating the flame.

Several experiments were conducted to establish the optimum fuel flow rate for maximum transmission, and the variation in percentage transmission with fuel flow. The results are shown in Figure 22. Transmission by an unshielded flame was negligible at 177.5 nm, and only one or two percent at the other lines.

No background emission from the flame was detected at these wavelengths.

4.5 Atomic absorption characteristics of phosphorus at the 177.5 nm line

It was found that absorption did in fact occur at the 177.5 nm line when phosphate solutions were sprayed into a sep-

FIGURE 22

FLAME TRANSMISSION CURVES FOR THREE PHOSPHORUS LINES

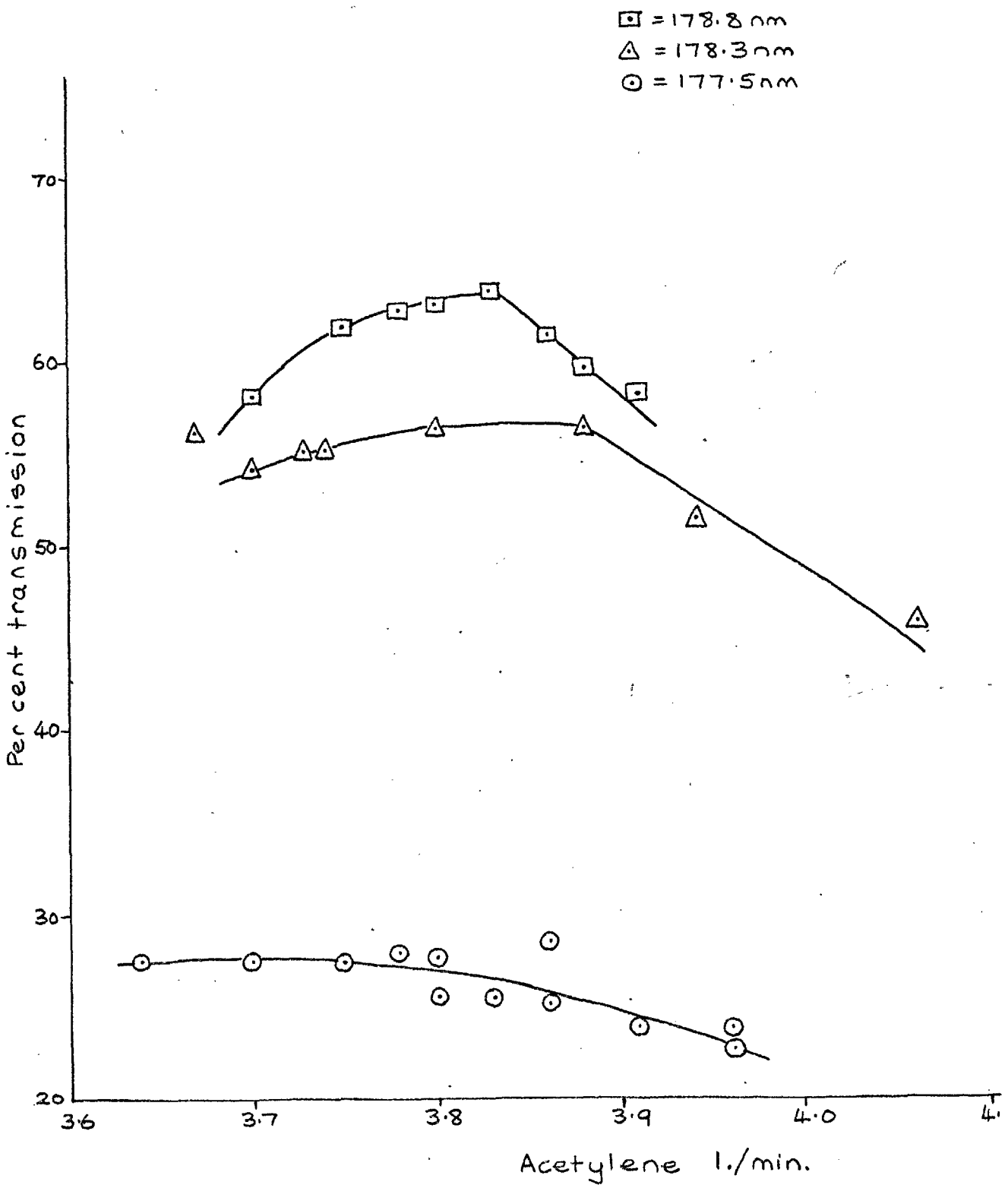

arated nitrous oxide-acetylene flame. Previous experiments where phosphate solution was found not to absorb at the sulphur 180.7 nm line in similar circumstances lent support to the view that this absorption was due to the presence of phosphorus atoms, rather than any other cause. The absorbance produced was found to be linearly proportional to the concentration of phosphorus present, and a calibration graph was plotted over the range 80 - 600 mg phosphorus /l (see Figure 23). No phosphorus atomic emission from the flame could be detected.

In order to calculate the mean absorption sensitivity, a solution containing 200 mg/l phosphorus was sprayed repeatedly and the mean absorbance calculated (see Table 10). Similarly, the detection limit (that concentration for which the relative standard deviation equals fifty percent) was calculated from repeated absorbance measurements on a solution containing 40 mg/l phosphorus (see Table 11). These procedures were based on the recommendations of the Society for Analytical Chemistry (60).

Table 10

Mean absorption sensitivity at 177.5 nm

Concentration	Absorbance
200 mgP/l	0.1935
" "	0.1915
" "	0.1665
" "	0.1525
" "	0.1751
" "	0.2018
Mean absorbance =	0.1802

Mean sensitivity = 4.8 mg P/l / 1% absorption

FIGURE 23

CALIBRATION CURVE FOR PHOSPHATE IN THE $N_2O-C_2H_2$ FLAME AT 177.5NM

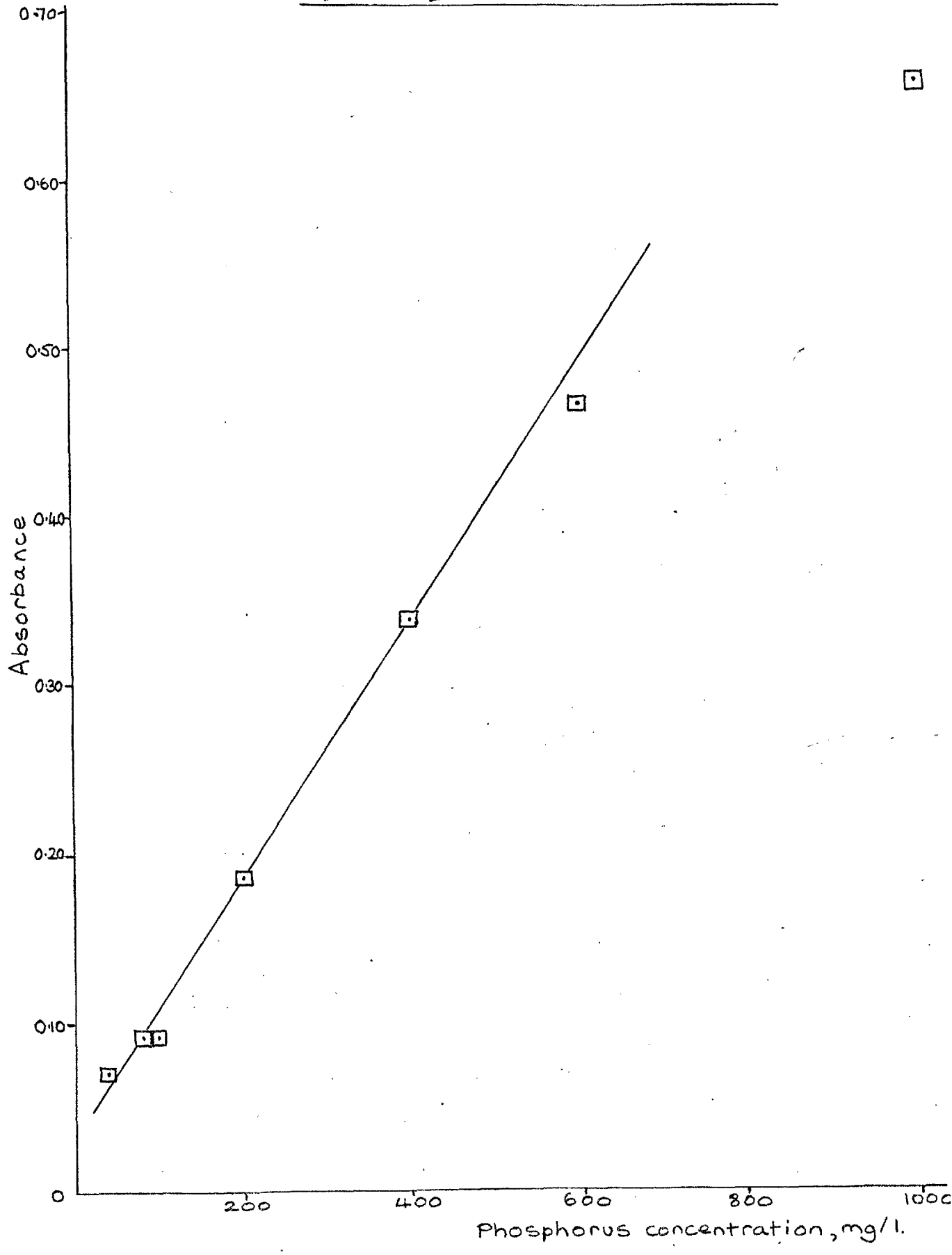

Table 11

Detection limit at 177.5 nm

Concentration	Absorbance
40 mg P/l	0.0309
" "	0.0185
" "	0.0302
" "	0.0520
" "	0.0338
" "	0.0219
" "	0.0497
" "	0.0355
" "	0.0405
" "	0.0661
Mean absorbance =	0.0379

Relative standard deviation = ± 36.4%

Detection limit = 29 mg P/l

4.6 Atomic absorption characteristics of phosphorus at the 178.3 nm line

No phosphorus atomic emission was observed at this line, as shown by the results of a typical experiment quoted in Table 12.

Table 12

Emission measurements at 178.3 nm

Condition	Total counts
Dark current	1334
Water	1291
1000 mg P/l	1270

However atomic absorption was observed at this spectral line, and a plot of absorbance versus phosphorus concentration is

shown in Figure 24. The mean sensitivity and detection limit were calculated as before, and the results are tabulated below (see Tables 13 and 14).

Table 13

Mean absorption sensitivity at 178.3 nm

Concentration	Absorbance
200 mg P/l	0.1592
" "	0.1616
" "	0.1592
" "	0.1633
" "	0.1671
" "	0.1590
Mean absorbance =	0.1616

Mean sensitivity = 5.4 mg P/l / 1% absorption

Table 14

Detection limit at 178.3 nm

Concentration	Absorbance
40 mg P/l	0.0433
" "	0.0240
" "	0.0161
" "	0.0370
" "	0.0307
" "	0.0328
" "	0.0331
Mean absorbance =	0.0310

Relative standard deviation = ± 26.3%

Detection limit = 21 mg P/l

It is interesting to note that although the absorption sensitivity was slightly greater at the 177.5 nm line, the 178.3 nm

FIGURE 24

CALIBRATION CURVE FOR PHOSPHATE IN THE $N_2O-C_2H_2$ FLAME AT 178·3NM

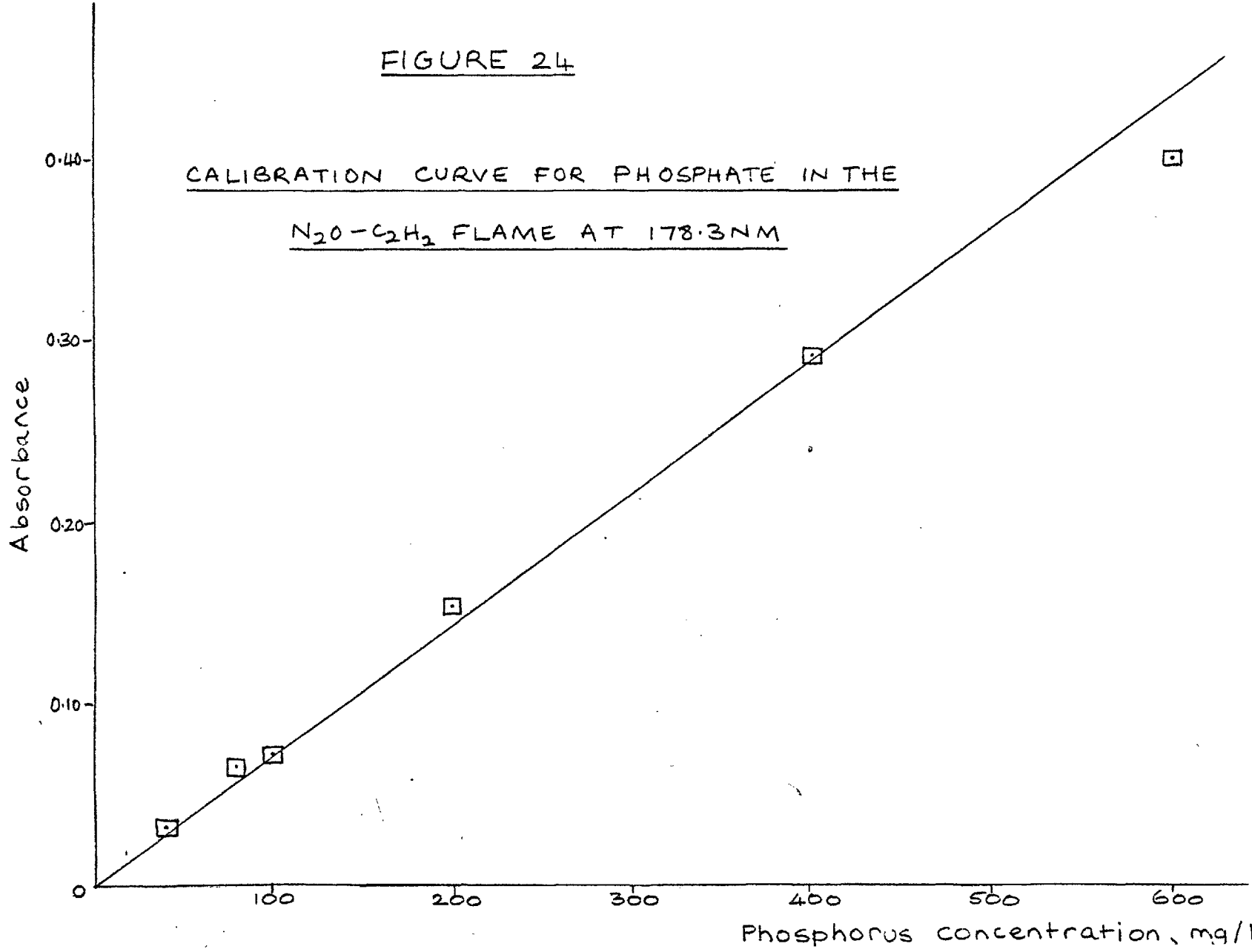

line gave the better detection limit.

4.7 Atomic absorption characteristics of phosphorus at the 178.8 nm line

A calibration curve for phosphorus atomic absorption at the 178.8 nm line is shown in Figure 25. The results of mean sensitivity and detection limit measurements made in the same manner as before are given in Tables 15 and 16.

Table 15

Mean absorption sensitivity at 178.8 nm

Concentration	Absorbance
200 mg P/l	0.0887
" "	0.0935
" "	0.0895
" "	0.0910
" "	0.0954
" "	0.1370
Mean absorbance =	0.0992

Mean sensitivity = 8.8 mg P/l / 1% absorption

FIGURE 25

CALIBRATION CURVE FOR PHOSPHATE IN THE $N_2O-C_2H_2$ FLAME AT 178·8 NM

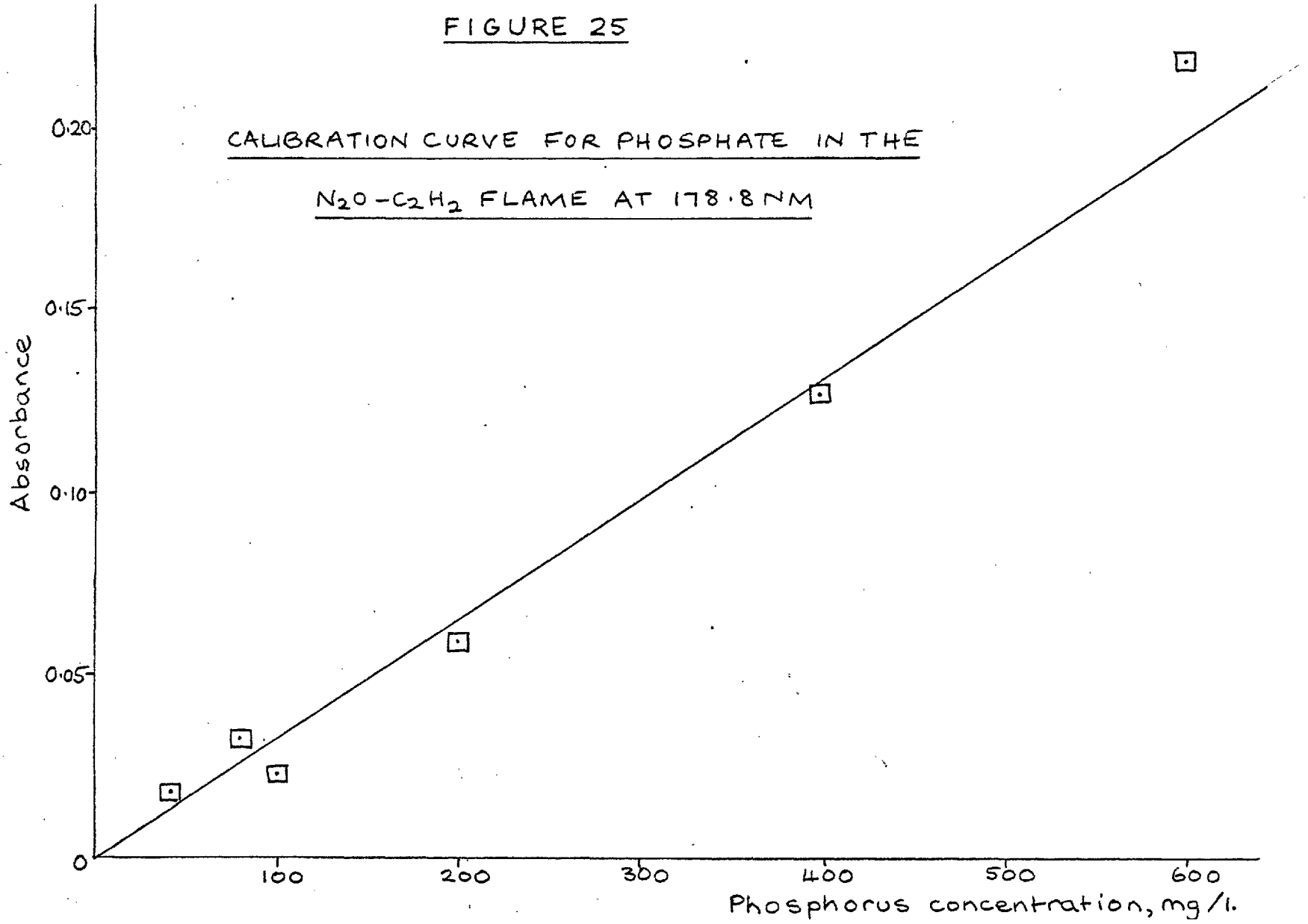

Table 16

Detection limit at 178.8 nm

Concentration	Absorbance
40 mg P/l	0.0172
" "	0.0027
" "	0.0184
" "	0.0068
" "	0.0235
" "	0.0119
" "	0.0094
" "	0.0222
" "	0.0156
" "	0.0257
Mean absorbance =	0.0153

Relative standard deviation = ± 46.7%

Detection limit = 37 mg P/l

No atomic emission was detected.

4.8 Discussion of the detection limits at the three lines

The above results show that the lowest detection limit is obtained at the 178.3 nm line. One factor which might influence this is the much greater radiation intensity reaching the detector at this wavelength, compared to the intensity of the 177.5 nm line. As noted before the relative emission intensities were approximately 5.6 : 1; this figure has also to be adjusted for the differing flame transmission factors, yielding a ratio at the detector, with the flame on, of about 15: 1. If, therefore, the noise in the absorbance measurement, expressed as the detection limit, were purely governed by the Poisson statistics of photon counting, we might expect a detection limit ratio at the two lines of $\sqrt{15} \times 4.8/5.4$: 1. The fact that this is not observed suggests that other noise factors may be more

important than the perceived photon flux in determining the detection limit. Noise factors which are likely to be important include turbulence in the flame and shielding gas leading to variable air entrainment, variations in the nebuliser's efficiency and fluctuations in the microwave power applied to the electrodeless discharge lamp.

4.9 Selection of the most useful line for analysis

The simplest and most common method of assessing the relative merits of the three lines would be to compare the detection limits. It should be realised however that the detection limit is by no means a perfect criterion of analytical utility. A more useful assessment could be made from a plot of relative standard deviation against solution concentration, since this would allow the analytical chemist to compare directly the relative standard deviations in the expected working range of the method. Such plots are, however, exceedingly tedious to construct, and so in this study a slightly simpler method was used.

Observation of the absorbances measured at the three lines for repeated sprayings of solution containing 200 mg/l phosphorus (Tables 10, 13, 15) yielded a set of relative standard deviations for the three lines at this concentration. These values, together with the detection limits, are tabulated below.

Table 17

Some precision data for the three phosphorus lines

Wavelength	Detection limit	Relative standard deviation at 200 mg P/l
177.5 nm	29 mg P/l	± 9.5%
178.3 nm	21 mg P/l	± 1.8%
178.8 nm	37 mg P/l	± 20.5%

From the data in Table 17, it was clear that the 178.3 nm line should be chosen. It seems however that this choice is in part a result of instrumental factors, and it may well be

that a more perfect instrument might more effectively use the greater sensitivity of the 177.5 nm line.

4.10 Interference studies

Another important criterion of the utility of an analytical method is its selectivity. The selectivity of the atomic absorption spectrochemical determination of phosphorus was studied by investigating the effects of diverse ions on the absorbance measurements. Results for numerous common cations and anions are given in Table 18.

As can be seen, none of these common ions caused any measurable interference where all differences less than three times the relative standard deviation are regarded as insignificant.

The situation with iodine (present as potassium iodide) was somewhat more complex. Table 19 gives the results of interference measurements made at all three phosphorus lines.

Table 19

Effect of 5000 mg/l iodine on 150 mg/l phosphorus

Wavelength	% Difference	R.S.D.	% Difference/R.S.D.	Interference?
178.8 nm	- 5.0	8.7	- 0.58	No
178.3 nm	+ 77.3	6.4	+ 12.0	Yes
177.5 nm	- 22.7	35.2	- 0.64	No

Since there is no interference at the 177.5 nm or 178.8 nm lines the iodine cannot be influencing the processes of phosphorus atom formation through some chemical mechanism. It is therefore likely that the effect is spectroscopic in nature. A study of the Grotrian diagram for iodine (33) reveals a resonance line of wavelength 178.276 nm. The spacing between this line and the 178.287 nm line of phosphorus is rather greater than would be expected for overlap to occur, particularly when it is remembered that half-widths of emission lines from hollow cathode lamps are generally about 0.001 nm (61). It is possible that there is some error in the wavelengths quoted, as

Table 18

Effect of foreign ions on the determination of phosphorus at 178.3 nm

Foreign ion	Concentration mg/l	Phosphorus Concentration mg/l	%Difference	R.S.D.	%Difference / R.S.D.
Na^{+}	5000	100	- 0.3	15.7	- 0.0002
Ca^{2+}	5000	100	- 5.4	15.7	- 0.34
Mg^{2+}	10000	200	+ 3.6	5.8	+ 0.62
B^{3+} ≠	5000	150	+ 6.0	8.4	+ 0.71
Ba^{2+}	5000	150	- 6.9	8.4	- 0.82
Zn^{2+}	5000	150	- 2.3	7.8	- 0.29
Co^{3+}	5000	150	+ 6.2	8.5	+ 0.73
Li^{+}	5000	150	- 0.9	2.6	- 0.36
Ni^{2+}	5000	150	+ 0.3	10.6	+ 0.03
*S	5000	150	- 7.8	8.2	- 0.95
Al^{3+}	5000	150	+ 18.5	7.0	+ 2.63
Mg^{2+}	5000	150	+ 4.5	6.8	+ 0.67
Cr^{3+}	5000	150	+ 3.0	5.0	+ 0.61
Cu^{2+}	5000	150	- 1.5	5.6	- 0.27
Mo	5000	150	- 1.3	4.0	- 0.33
Cl^{-}	5000	150	- 4.3	5.2	- 0.83
Br^{-}	5000	150	- 0.2	5.2	- 0.04
F^{-}	5000	150	- 5.2	5.2	- 0.99
NO_3^{-}	5000	150	+ 4.0	5.7	+ 0.70
$EDTA^{2-}$	5000	150	+ 8.0	5.7	+ 1.40
CO_3^{2-}	5000	150	+ 11.0	5.7	+ 1.93

R.S.D. = relative standard deviation of standard solution

* = S as SO_4^{2-}

≠ = B as BO_3^{3-}

such measurements are rather difficult and not very accurate in the vacuum ultra-violet. However, it is known that iodine emission lines are very prone to self-absorption and pressure broadening, so similarly wide absorption line profiles might also be expected. Equally, of course, the emission line from the phosphorus electrodeless discharge lamp may be rather broad.

One interesting possibility which results from this spectral overlap is that an iodine electrodeless discharge lamp might be used as the spectral source for atomic absorption of phosphorus at 178.3 nm. This might well prove advantageous, as iodine electrodeless discharge lamps are much more intense and stable than those of phosphorus. The absorption sensitivity obtained would depend fairly critically on the line profiles of the source and absorbing atoms, but in this case the Lindholm theory of line broadening (10) predicts that the shifts due to collisional processes should be in such a direction as to give greater overlap.

This particular spectral interference by iodine on the 178.3 nm line is unlikely to be of significance for the majority of analyses, but if a particular sample is known to contain very large amounts of iodine, then obviously it would be necessary to carry out the determination at the 177.5 nm line.

4.11 Determination of phosphorus in some foodstuffs

Phosphorus is an essential nutritional material (62), and in consequence it frequently has to be determined in foodstuffs. The normal method adopted consists of a wet ashing procedure followed by a "moybdenum blue" type of colorimetric determination (63).

Inevitably the necessity to wet ash the sample in order to obtain a colourless digest makes the procedure lengthy and tedious. In these circumstances the atomic absorption spectrochemical method would appear to have considerable advantages for any readily soluble material. It was decided to test the technique using samples of dried milk powder, beef extract and yeast extract whose phosphorus contents had previously been measured by means of wet ashing followed by a molybdenum blue

determination using a Technicon AutoAnalyser (63).

Procedure

A small quantity (3 - 5 g) of the sample was weighed out, dissolved in either hot or cold distilled water, as appropriate, and made up to 100 ml. Two aliquots (40 ml each) were taken from this solution, to one a standard addition of phosphate solution (equivalent to 100mg P/l) was made, and the aliquots diluted to 100 ml.

The absorbances of the final solutions were measured in the separated nitrous oxide-acetylene flame at 178.3 nm, and hence the phosphorus content of the original sample calculated.

Results and discussion

The results obtained by the atomic absorption spectrochemical method, together with the comparison AutoAnalyser values are given in Table 20.

Some difficulty was experienced with the milk solutions, as these tended to deposit solid in the burner slot, causing it to block. It is probable that this tendency would be reduced if the concentration of the solutions used could be reduced. No such problems were encountered with the other sample solutions. It should be stressed that the build up of such solid deposits, and carbonisation, on burner slots is substantially reduced if the burner is cleaned thoroughly before use. Presumably any dirt present provides growth centres in an analogous process to the seeding of supersaturated solutions to provoke crystallisation.

As can be seen from Table 20, reasonable agreement was obtained between the atomic absorption and AutoAnalyser methods, with the former technique giving slightly higher results. Relative standard deviations were also higher with the atomic absorption technique. When it is remembered that these results were obtained with a fairly crude, laboratory built apparatus, the agreement obtained suggests that the atomic absorption spectrochemical analysis method may have considerable promise for the determination of phosphorus in foodstuffs.

Table 20

Phosphorus content of some foodstuffs

Sample	AutoAnalyser			Atomic absorption			% Difference
	%P	Mean	R.S.D. %	%P	Mean	R.S.D. %	
Yeast extract	1.32 1.34 1.31 1.19	1.29	5.37	1.43 1.32 1.27	1.34	6.17	+ 3.88
Beef extract	0.714 0.726 0.740 0.696	0.719	2.57	0.738 0.704 0.749	0.730	3.26	+ 1.53
Milk powder	1.02 0.975 0.991 0.955	0.985	2.81	1.00 1.12 1.13	1.08	6.62	+ 9.98

4.12 Other possible applications

The determination of phosphorus by atomic absorption spectrometry, as described above, is neither as sensitive nor as precise as some of the colorimetric procedures which are available for phosphorus determination. However the technique is inherently more selective than colorimetric procedures; it avoids the need to obtain a colourless digest of the sample; it may also, because of the avoidance of wet ashing, result in a saving of the chemist's time, and reduce the degree of skill required to obtain accurate results.

There are a number of materials containing fairly large amounts of phosphorus, where the selectivity of the determination is more critical than the sensitivity. Examples include foodstuffs, fertilizers, ores, slags, rocks, phosphor-bronze alloys and detergents.

It seems likely that this technique could be applied to such materials with reasonable success.

CHAPTER 5

THEORETICAL SENSITIVITY OF ATOMIC ABSORPTION SPECTROMETRY

It is possible to calculate the atomic absorption sensitivity which should be attained for a given line of a particular element, provided that the transition probability and oscillator strength are known (8, 10). The process will be illustrated for the cases of the sulphur 180.7 nm line and the phosphorus 177.5 nm line, assuming that the spectral source is perfectly monochromatic, that the flame gases behave ideally, and that, in the case of phosphorus, the effect of hyperfine splitting may be ignored.

5.1 Effect of broadening processes on the line width

It is necessary first to calculate the effect of the various broadening processes upon the absorption line. The important processes in a flame are Doppler broadening and collisional broadening. Lorentz's method will be used to calculate the latter since, although incorrect, it is sufficiently accurate for the purpose; the natural half-widths will also be calculated for completeness, although they are insignificant in relation to the other factors.

5.2 Natural half-width

The natural half-width of a line is a result of the finite lifetimes of the energy states involved, and is an example of Heisenberg's uncertainty principle. For a resonance line the determining factor is the lifetime of the upper state, since the lifetime of the ground state is effectively infinite. The relation is

$$\Delta\nu_N = \frac{1}{2\pi\tau} \qquad \text{sec}^{-1} \qquad 5.1$$

(The meaning of all the symbols used in this discussion is given in Table 21).

By definition, the transition probability A_{ki} is the reciprocal

Table 21

Symbols, definitions and units for sensitivity calculations

Symbol	Definition	Unit
A	Absorbance	
A_{Ri}	Transition probability	sec^{-1}
A_W	Atomic weight of absorbing atom	amu
α'	Damping constant	
α	Degree of dissociation of absorbing atoms	
C	Concentration of absorbing atoms in solution	mg/l
c	Velocity of light	cm/sec
e	Electronic charge	esu
η	Molar ratio of combustion products to reactants	
ε	Nebuliser efficiency	
$\Delta\nu_D$	Doppler half-width	sec^{-1}
$\Delta\lambda_D$		nm
$\Delta\nu_L$	Lorentz half-width	sec^{-1}
$\Delta\lambda_L$		nm
$\Delta\nu_N$	Natural half-width	sec^{-1}
$\Delta\lambda_N$		nm
f	Oscillator strength	
g_i	Statistical weight of ith level	
Σg_o	Sum of statistical weights of multiplet	
k_ν	Overall absorption coefficient	cm^{-1}
$k_{o(D)}$	Absorption coefficient for pure Doppler broadening	cm^{-1}
l	Flame pathlength	cm
λ	Wavelength	nm
M	Effective molecular weight of flame gases	amu
m	Electronic mass	g

Table 21 (continued)

Symbol	Definition	Unit
N_A	Number of absorbing atoms per unit volume	cm^{-3}
N_F	Number of foreign molecules per unit volume	cm^{-3}
ν	Frequency	sec^{-1}
ν_o	Frequency at line centre	sec^{-1}
p	Pressure of gas in flame	mm Hg
R	Universal gas constant	erg/mole/^oK
S	Solution flow rate into nebuliser	cm^3/min
σ_L	Collision cross section	cm
T	Flame temperature	^oK
τ	Life time of electron in upper state	sec
V_g	Volume of burnt flame gases	cm^3
V	Flow rate of gases to flame	cm^3/min

of the lifetime.

$$\therefore \Delta\nu_N = \frac{A_{ki}}{2\pi} \quad sec^{-1} \qquad 5.2$$

5.3 Lorentz half-width

The Lorentz half-width is given by

$$\Delta\nu_L = \frac{\text{Number of collisions per absorbing atom per second}}{\pi} \qquad 5.3$$

$$\therefore \Delta\nu_L = \frac{2}{\pi} \cdot \sigma_L^2 \cdot N_F \sqrt{2\pi RT\left(\frac{1}{A_W} + \frac{1}{M}\right)} \quad sec^{-1} \qquad 5.4$$

$$\text{but} \quad N_F = \frac{9.740 \times 10^{18}}{T} \cdot P \qquad 5.5$$

$$\therefore \Delta\nu_L = 1.417 \times 10^{22} \cdot p \cdot \sigma_L^2 \sqrt{\frac{1}{T}\left(\frac{1}{A_W} + \frac{1}{M}\right)} \quad sec^{-1} \qquad 5.6$$

5.4 Doppler half-width

The Doppler half-width may be calculated using the formula

$$\Delta\nu_D = \frac{2\sqrt{2R\ln 2}}{c} \cdot \nu_0 \sqrt{\frac{T}{A_W}} \quad sec^{-1} \qquad 5.7$$

Substituting for the various constants gives

$$\Delta\nu_D = 7.16 \times 10^{-7} \nu_0 \sqrt{\frac{T}{A_W}} \quad sec^{-1} \qquad 5.8$$

The half-widths so calculated may be converted into wavelength units using the relations

$$d\lambda = \frac{c}{\nu^2} \cdot d\nu = \frac{\lambda^2}{c} \cdot d\nu \qquad 5.9$$

5.5 Calculation of the Voigt integral

The half-widths so obtained can then be employed to calculate the damping constant

$$a' = \frac{\Delta\nu_N + \Delta\nu_L}{\Delta\nu_D} \qquad 5.10$$

Voigt showed (8) that the profile of an absorption line subject to natural, Lorentz and Doppler broadening could be described by

$$\frac{k_\nu}{k_{o(D)}} = \frac{a'}{\pi} \int_{-\infty}^{\infty} \frac{e^{-y^2}\, dy}{a'^2 + (\omega - y)^2} \qquad 5.11$$

where $$\omega = \frac{2(\nu - \nu_o)}{\Delta \nu_D} \sqrt{\ln 2}$$

and $$y = \frac{2\delta}{\Delta \nu_D}$$

δ being the frequency displacement from $(\nu - \nu_o)$. For small values of a', Reiche demonstrated (8) that the Voigt integral simplified to

$$\frac{k_\nu}{k_{o(D)}} = \exp^{-\omega^2} - \frac{2a'}{\sqrt{\pi}} \left[1 - 2\omega F(\omega)\right] \qquad 5.12$$

For idealised atomic absorption, $\omega = 0$, therefore $F(\omega) = 0$ also, so equation 5.12 becomes

$$\frac{k_\nu}{k_{o(D)}} = 1 - \frac{2a'}{\sqrt{\pi}} \qquad 5.13$$

However for the more usual case where the damping constant is large, the Voigt integral must be solved numerically. Additionally the value of the integral must be corrected for the effect of the line shift, using the quantum mechanical theory of collisional broadening. This has been carried out by L'vov (10) whose results are given in Table 22.

Table 22

Values of the Voigt integral allowing for line shift

a'	$k_\nu / k_{o(D)}$
10	0.0368
2	0.192
1.5	0.248
1.0	0.356
0.5	0.569

5.6 Calculation of theoretical sensitivity

Now $k_{o(D)}$, the absorption coefficient for a line subject only to Doppler broadening, is related to the number of absorbing atoms per unit volume, and the oscillator strength by

$$k_{o(D)} = \frac{2}{\Delta\nu_D}\sqrt{\frac{\ln 2}{\pi}} \cdot \frac{\pi e^2}{mc} \cdot N_A \cdot f \qquad 5.14$$

and N_A is related to the rate of nebulisation of solution into the flame by

$$N_A = \frac{6{\cdot}02 \times 10^{23} \times C \times S \times \alpha \times \varepsilon \times g_i}{A_W \times V_g \times \Sigma g_o} \qquad 5.15$$

where it is assumed that for multiplet ground states the population given by the Boltzman distribution is proportional to the statistical weight of each level. For singlet ground states the term $\frac{g_i}{\Sigma g_o}$ becomes unity. The volume of the flame gases, V_g, is obtained by allowing for the relative volumes of the flame gases before and after combustion, η, and the increased flame temperature, T. Thus

$$V_g = \frac{V T \eta}{300} \qquad 5.16$$

and so

$$N_A = \frac{6{\cdot}02 \times 300 \times 10^{23} \times C \times S \times \alpha \times \varepsilon \times g_i}{A_W \times V \times T \times \eta} \qquad 5.17$$

Also, the absorbance, A, is given by

$$A = 0{\cdot}4343\, k_\nu \cdot l \qquad 5.18$$

and therefore

$$A = \frac{k_\nu}{k_{o(D)}} \cdot \frac{C.S.\alpha.\varepsilon.f.l.g_i}{\Delta\nu_D.A_W.V.T.\eta.\Sigma g_o} \cdot 2\sqrt{\pi \ln 2}\,\frac{e^2}{mc}.0{\cdot}4343 \times 6{\cdot}02 \times 3 \times 10^{25} \qquad 5.19$$

Sensitivity is usually defined in terms of concentration (in mg/l) required to produce 1% absorption (A = 0.00436). Substituting for constants and rearranging equation 5.19 yields the following expression for sensitivity

$$\text{Sensitivity} \atop (\text{mg/l / 1\% absorption}) = \frac{1}{\left(k_\nu / k_{o(D)}\right)} \cdot \frac{\Delta\nu_D.A_W.V.T.\eta.\Sigma g_o}{S.\alpha.\varepsilon.f.l.g_i} \times 2236 \times 10^{-20} \qquad 5.20$$

where the symbols have the meanings assigned in Table 21.

Equation 5.20 allows the calculation of atomic absorption sensitivity directly from the properties of the atom.

5.7 Practical assumptions

The main difficulties are the selection of values for the flame temperature, the effective molecular weight of the flame gases and the collision cross section. A mean molecular weight of 21.67 will be adopted for a nitrous oxide-acetylene flame, following the composition calculated by Taylor (30), and a flame temperature of 2800°K will be assumed, after Kirkbright and Vetter (64). The flame gas pressure is taken as 760 mm Hg. Winefordner (65) discussed the problem of collisional cross sections and calculated two values of Lorentz broadening, using 20×10^{-16} cm^2 and 100×10^{-16} cm^2 to allow for the best and worst cases respectively. These values will also be assumed here.

5.8 Sensitivity calculations for the sulphur 180.7 nm line and the phosphorus 177.5 nm line

For the 180.7 nm line of sulphur, equation 5.2 gives

$$\Delta\nu_N = \frac{4.1 \times 10^8}{6.284} \quad \text{sec}^{-1}$$

$$\therefore \Delta\nu_N = 6.53 \times 10^7 \quad \text{sec}^{-1}$$

and $$\Delta\lambda_N = 0.071 \times 10^{-4} \quad \text{nm}$$

Substitution in equation 5.8 yields

$$\Delta\nu_D = \frac{7.16 \times 10^{-7} \times 3 \times 10^{10}}{180 \times 10^{-7}} \sqrt{\frac{2800}{32.064}} \quad \text{sec}^{-1}$$

$$\therefore \Delta\nu_D = 1.111 \times 10^{10} \quad \text{sec}^{-1}$$

and $$\Delta\lambda_D = 1.209 \times 10^{-3} \quad \text{nm}$$

whilst equation 5.6 shows that

$$\Delta\nu_{L(min)} = 1.417 \times 10^{22} \times 760 \times 20 \times 10^{-16} \sqrt{\frac{1}{2800}\left(\frac{1}{32.064} + \frac{1}{21.67}\right)} \quad \text{sec}^{-1}$$

$$\therefore \Delta\nu_{L(min)} = 1.132 \times 10^9 \quad \text{sec}^{-1}$$

and $$\Delta\lambda_{L(min)} = 1.232 \times 10^{-4} \quad \text{nm}$$

Similarly

$$\Delta\nu_{L(max)} = 5.659 \times 10^9 \quad \text{sec}^{-1}$$

and $$\Delta\lambda_{L(max)} = 6.162 \times 10^{-4} \quad \text{nm}$$

Thus, from equation 5.10

$$a'_{(max)} = 0.43$$

and $$a'_{(min)} = 0.09$$

Taking the worst case, and assuming that $a'_{(max)} \simeq 0.5$, then Table 22 gives the Voigt integral as 0.569. Substitution of the above values, together with those in Table 23, into equation 5.20 gives

$$\text{Sensitivity} = \frac{2.236 \times 10^{-20} \times 1.111 \times 10^{10} \times 32.064 \times 12.4 \times 10^{3} \times 2800 \times 1.667 \times 9}{0.569 \times 6.5 \times 1 \times 0.1 \times 0.12 \times 7 \times 5}$$

$\therefore$ Sensitivity = 2.7 mg/l / 1% absorption.

Table 23

Flame parameters for sensitivity calculations

V	= 12.4 10^3 cm^3/min
T	= 2800°K
η	= 1.667
S	= 6.5 cm^3/min
α	= 1.0
ε	= 0.10
l	= 7 cm

Similar calculations were performed for the phosphorus 177.5 nm line, ignoring the hyperfine splitting; the results are given in Table 24.

5.9 Comparison of calculated and experimental sensitivities

Comparison of the calculated values with the experimental values shows the latter to be somewhat lower. Thus for sulphur a sensitivity of 9.0 mg/l / 1% absorption was obtained, compared with the calculated value of 2.7; for phosphorus at the 177.5 nm line the calculated and experimental values were 3.5 and 4.8 mg/l / 1% absorption respectively.

A number of reasons may be given to account for this discrepancy:

1. The shielding gas may dilute the atomic vapour in the

Table 24

Calculated results for phosphorus

$\Delta\nu_N$	$= 3.543 \times 10^{7}$ sec^{-1}
$\Delta\lambda_N$	$= 3.63 \times 10^{-6}$ nm
$\Delta\nu_{L(min)}$	$= 1.122 \times 10^{9}$ sec^{-1}
$\Delta\lambda_{L(min)}$	$= 1.178 \times 10^{-4}$ nm
$\Delta\nu_{L(max)}$	$= 5.611 \times 10^{9}$ sec^{-1}
$\Delta\lambda_{L(max)}$	$= 5.892 \times 10^{-4}$ nm
$\Delta\nu_D$	$= 1.150 \times 10^{10}$ sec^{-1}
$\Delta\lambda_D$	$= 1.208 \times 10^{-3}$ nm
$a'_{(min)}$	$= 0.10$
$a'_{(max)}$	$= 0.49$
Sensitivity using $a'_{(max)}$	= 3.5 mg/l /1% absorption

flame. No allowance has been made for this possibility.

2. The estimated nebuliser efficiency, ε, (= 0.1) may be incorrect.

3. The spectral source is unlikely to be perfectly monochromatic, so that the absorption coefficient should be calculated over the emission line profile rather than at the centre of the absorption line. This would have the effect of reducing the overall absorption coefficient.

4. It has been assumed that the atomic vapour is uniformly distributed in space, and that the path of the light beam is completely within the absorbing cloud; this is probably unrealistic.

CHAPTER 6

DISCUSSION

The preliminary studies in analytical atomic spectroscopy below two hundred nanometres presented here indicate that the technique of atomic absorption spectrometry may be used for the determination of elements with short wavelength resonance lines.

The principal problem of devising an efficient atom cell, transparent to the short wavelength radiation involved, has been resolved with reasonable success. It has been shown that the carbon filament atom reservoir is unsuitable for the task; that the conventional air-acetylene flame lacks sufficient transparency, and that the hydrogen-nitrogen diffusion flame, though possessing moderate transparency, is inefficient in the generation of free atoms. Thus the most satisfactory of the atom cells studied was the nitrogen separated nitrous oxide-acetylene flame. This possessed very high transparency and was apparently very efficient in the generation of free atoms, as indicated by the relatively high absorption sensitivities and freedom from chemical interference effects.

A considerable amount of further study is required, however, before the problems of flame atomic absorption spectroscopy in this wavelength range can be regarded as solved. One desirable improvement in the technique would be a reduction in flame turbulence. This is an important source of low frequency noise which seriously degrades the detection limits obtained. Figures 14 and 22 indicate that small variations in the acetylene flow rate produce large changes in flame transparency at short wavelengths; similar considerations apply to the nitrous oxide and shielding gas flow rates, and these should all be closely controlled. The biggest improvement could probably be made in reducing shielding gas turbulence, since the very high flow rates involved here tend to promote turbulence. One possibility would be to replace the burner shield employed here, which was packed with crimped foil strip (27), with a better design made from a matrix of closely packed narrow capillaries (66).

This latter would give improved laminar flow of the shielding gas and so result in better flame separation. It might also prove possible to develop a different type of shielded burner, combining the concepts of the Smithells separator (26) and inert gas shielding. Figure 26 illustrates a possible design. Most of the disadvantages of the Smithells separator arise from the fact that the flame is in contact with the silica walls of the separator tube. If the burner was surrounded by a capillary shield, around which a Smithells separator was placed, so that a thin laminar flow of inert gas could be interposed between the flame and the silica tube, some of the disadvantages of the method might be overcome. Such a design would completely eliminate air entrainment, so removing one source of flame noise, but could only be conveniently applied to small round burners, rather than the long burners more useful in atomic absorption spectroscopy.

Some difficulty can be expected in extending the flame methods to even shorter wavelengths than the 177.5 nm reached in this work. Obviously the determination of carbon at 165.7 nm, for instance, will be difficult in a carbonaceous flame; although the technique should provide very useful information for studies of flame structure and combustion processes. Flame transparency at even lower wavelengths depends on the absorption spectra of the various molecular species present. This is rather an unknown quantity, but it is safe to say that exceedingly efficient steps would need to be taken to exclude entrained air from the flame cell, and this probably implies an improvement on present apparatus.

Other types of atom cell may be applicable to this spectral region, besides the flame cell and L'vov furnace, and some might be more suitable at these short wavelengths. Possibilities include Langmuir's atomic hydrogen torch (67) and the microwave excited plasma (53). It might also prove wise to reassess the usefulness of the radio-frequency excited argon plasma as an atom cell for atomic absorption and atomic fluorescence spectroscopy.

Other instrumental difficulties arise at about 165 nm, as a result of the increasing absorption by even high purity

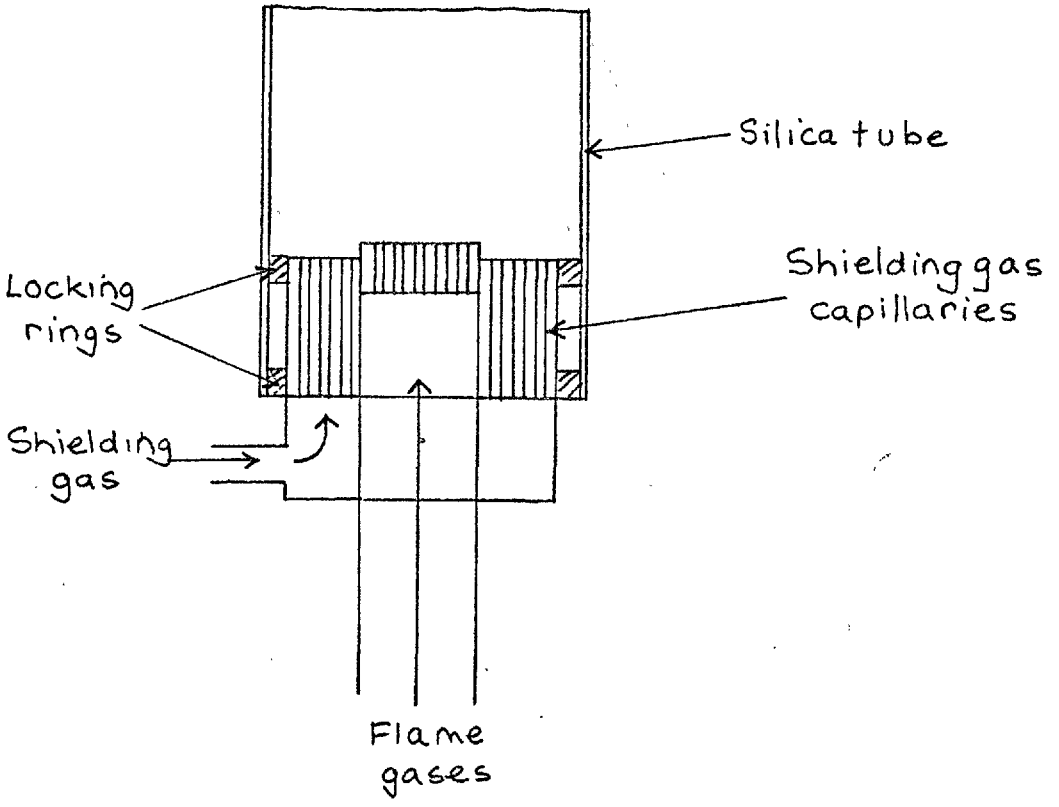

FIGURE 26

COMBINED SILICA-TUBE – INERT GAS SEPARATED BURNER

silica. This necessitates the employment of calcium or lithium fluoride glasses for optics and windows, including photomultiplier envelopes. More important, however, are likely to be the new techniques required for construction of spectral sources. Hollow cathode lamps for use in this spectral region are commercially available, though in view of the results obtained with a phosphorus hollow cathode lamp (Chapter 4) it is doubtful whether they would be satisfactory. Construction of electrodeless discharge lamps of the conventional type will be complicated by the opacity of silica; moreover it is not possible to simply replace silica with lithium fluoride as this becomes opaque when hot. Attempts have been made to construct a hydrogen electrodeless discharge lamp by attaching lithium fluoride windows to a silica lamp body (68) but this approach was not completely satisfactory. Various types of plasma have been used as sources of vacuum ultra-violet radiation (12), and some type of windowless, flow-through electrodeless discharge lamp may also be possible.

In this study, a vacuum monochromator was employed; it is, however, possible to employ a monochromator which is purged with inert gas, rather than evacuated. Such an approach is interesting, in that conventional atomic absorption spectrometers might be modified to extend their spectral range. The author, in conjunction with other workers, has converted two commercial atomic absorption instruments to permit their use in the vacuum ultra-violet.

In the first case, a Techtron AA4 spectrometer (Techtron Pty., Melbourne, Australia) was adapted by arranging to flush the monochromator with a constant stream of nitrogen, which effectively removed all air from the optical path. Using this instrument in conjunction with a radio-frequency induction-coupled argon plasma torch it has been found possible to determine phosphorus, sulphur, iodine and mercury at their vacuum ultra-violet lines by atomic emission. Improved detection limits for atomic emission were also observed for the arsenic and selenium lines below two hundred nanometres when the monochromator was purged (69, 70).

In the second case, a Perkin-Elmer 290B spectrometer (Per-

kin-Elmer Corp., Norwalk, Conn., U.S.A.) was adapted to provide a completely nitrogen purged optical path. This apparatus has been employed for the determination of iodine at 183 nm (40), and mercury at 184.9 nm (71), by atomic absorption in a separated nitrous oxide-acetylene flame.

Another approach is to eliminate the monochromator altogether, and use a non-dispersive system. One established method is the use of a "solar-blind" photomultiplier. This is a tube whose photocathode is constructed of emissive material having an unusually high work function. Consequently the tube only responds to light which is sufficiently energetic, and hence discriminates between light longer or shorter than a given wavelength. Although such systems have been tested for atomic fluorescence in the ordinary ultra-violet, as shown in Figure 27 (72), the degree of spectral isolation achieved is inadequate for most purposes. A range of sapphire window vacuum photodiodes is also available which possess a variety of spectral ranges, and appear attractive for use in non-dispersive systems.

It is possible to construct a variety of optical filters for use in the vacuum ultra-violet (12); the most promising technique is to exploit the absorption bands of molecular vapours. An example is the use of an oxygen filter for the hydrogen 121.5 nm line.

Equally, it is possible to construct photo-ionisation detectors with limited spectral responses (10, 12). Light of sufficiently short wavelength ionises molecular vapour contained in a cell, and the extent of ionisation is measured electrically, giving a measure of the light intensity (see Figure 28). Suitable matching of the vapour, whose ionisation potential sets the upper wavelength limit, with an appropriate window material, whose transmission cut-off sets the lower wavelength limit, makes it possible to produce detectors with a wide variety of spectral characteristics. As an example, an ionisation chamber filled with dimethylaniline vapour (ionisation potential 7.14 electron volts) will only respond to wavelengths below 174 nm. If such a chamber is fitted with an ultra-thin quartz window which is opaque below 150 nm, then the combined detector will have a spectral range of 150 - 174 nm. Another example

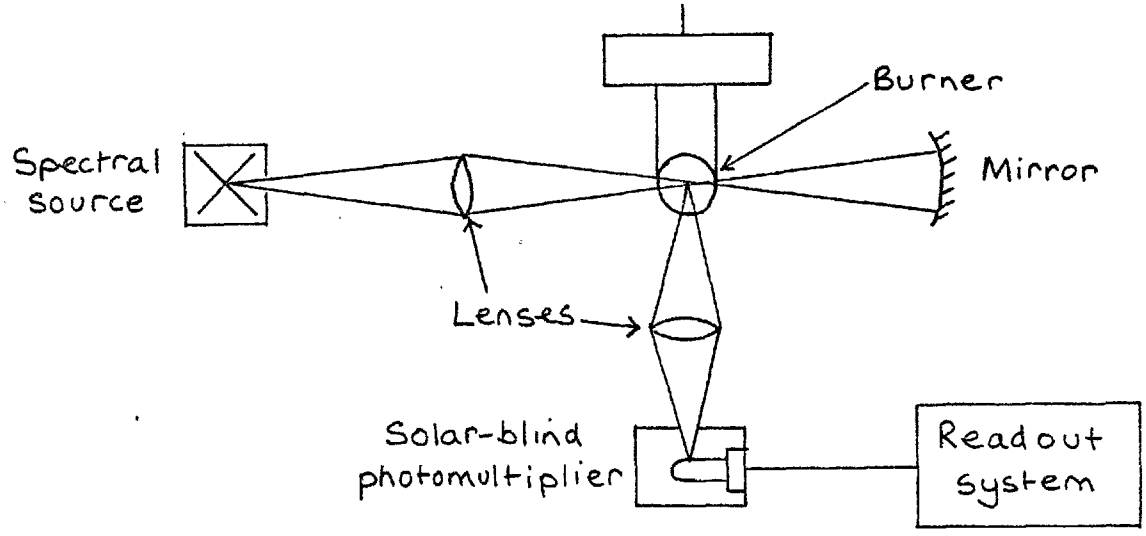

FIGURE 27

APPARATUS FOR ATOMIC FLUORESCENCE

USING A SOLAR-BLIND PHOTOMULTIPLIER

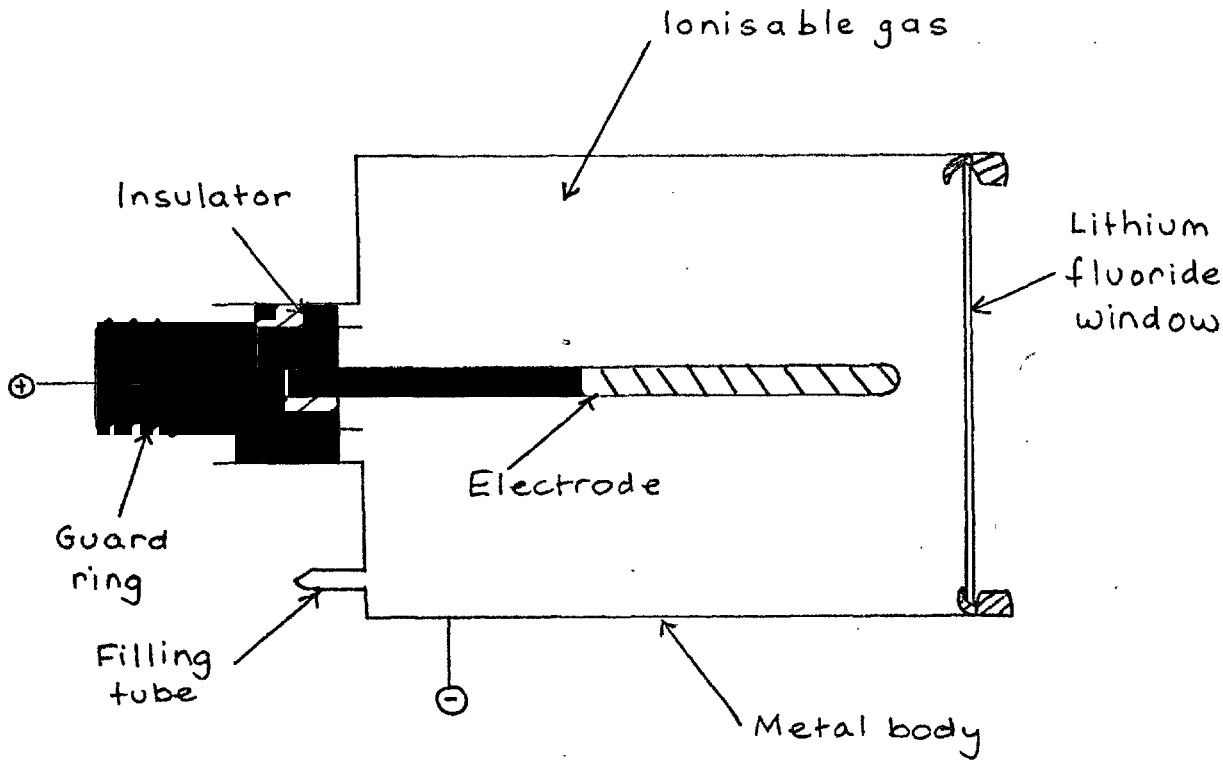

FIGURE 28

PHOTO-IONISATION CHAMBER

is the use of a chamber filled with nitric oxide coupled with a lithium fluoride window; this permits detection of the xenon resonance line at 129.5 nm, and covers the spectral range 130.4 -105 nm. It might also be possible to use two chambers, so that the first detected radiation shorter than, say, x nm, and the second, having a longer wavelength threshold, detected radiation below y nm. The readings could be combined to indicate the intensity in the range (x -y) nm.

One other non-dispersive detector whose applicability in the vacuum ultra-violet merits consideration is the resonance detector (73). The principle is that a cloud of atoms of the element being sought is maintained in a chamber. When light corresponding to that element's resonance lines is incident on the detector, the cloud of atoms therein absorbs its specific radiation, the atoms are excited to corresponding higher levels and then decay, emitting fluorescent radiation. The intensity of the fluorescence is proportional to the intensity of the incident rays. The main requirement is to maintain a cloud of free atoms in the detector. Walsh et al used sputtering processes like those in an ordinary hollow cathode lamp; thermal or photolytic processes are also feasible. In the case of mercury or the noble gases the vapour is naturally monatomic and no problem arises. Another interesting case is that of the halogens bromine, chlorine and iodine where atoms might be fairly easily generated by photolysis. For example, bromine with a bond dissociation energy of 46.1 Kcal/mole should be dissociated by light of wavelengths less than 619 nm; the actual population of bromine atoms formed would depend on the quantum yield at the particular wavelength employed. However the widespread use of photolysis in organic chemistry indicates that it is relatively easy to generate chemically significant concentrations of free atoms by photolytic processes. In view of the comparatively long wavelengths needed for photolysis it would be possible to use a solar blind photomultiplier which was unaffected by the light used for atom generation, but was sensitive to the atomic fluorescence. Apart from the obvious technique of employing an external lamp as a photolysis source, it might be possible to use electrically heated tungsten fila-

ments placed in a side-arm inside the body of the resonance detector, so increasing the photochemical efficiency of the device.

Many of the difficulties in this study have arisen from the fact that extremely low light levels were being measured. Two possible ways of overcoming these difficulties seem obvious:

1. To increase the light flux either by developing more intense spectral sources, or using optical systems of greater aperture such as the non-dispersive detectors discussed above.

2. To devise more efficient electronic measurement systems so as to make the best possible use of the signals obtained.

Three possible electronic measurement techniques have been investigated herein, namely dc measurement, lock-in amplifiers and photon counting. A fourth detection scheme which merits further study is the noise-voltage method (74). The principle is that the photomultiplier shot noise is proportional to the incident light. Figure 29 illustrates the technique. It will be recollected from the discussion in Chapter 3 that the output of a photomultiplier is a series of sharp, unidirectional pulses. At high light levels the signal appears to consist of a dc current together with an ac component, generally regarded as "noise". It is clear that as the light level is reduced the ac component of the signal must form an ever increasing proportion of the output signal, until the limiting case is reached where separate pulses are obtained. Thus at low light levels the ac component of the signal may contain more power than the dc component, and it will therefore become advantageous to measure the ac component or "noise-voltage". Alfano and Ockman, who compared this technique with phase sensitive detection and photon counting, found that its sensitivity lay between that of the other two methods; they also suggested that the use of pulse height discrimination to set a minimum threshold level, as in photon counting, would improve the method's signal-to-noise ratio even further.

This work has elucidated some of the problems of atomic absorption spectrometry in the vacuum ultra-violet, and also

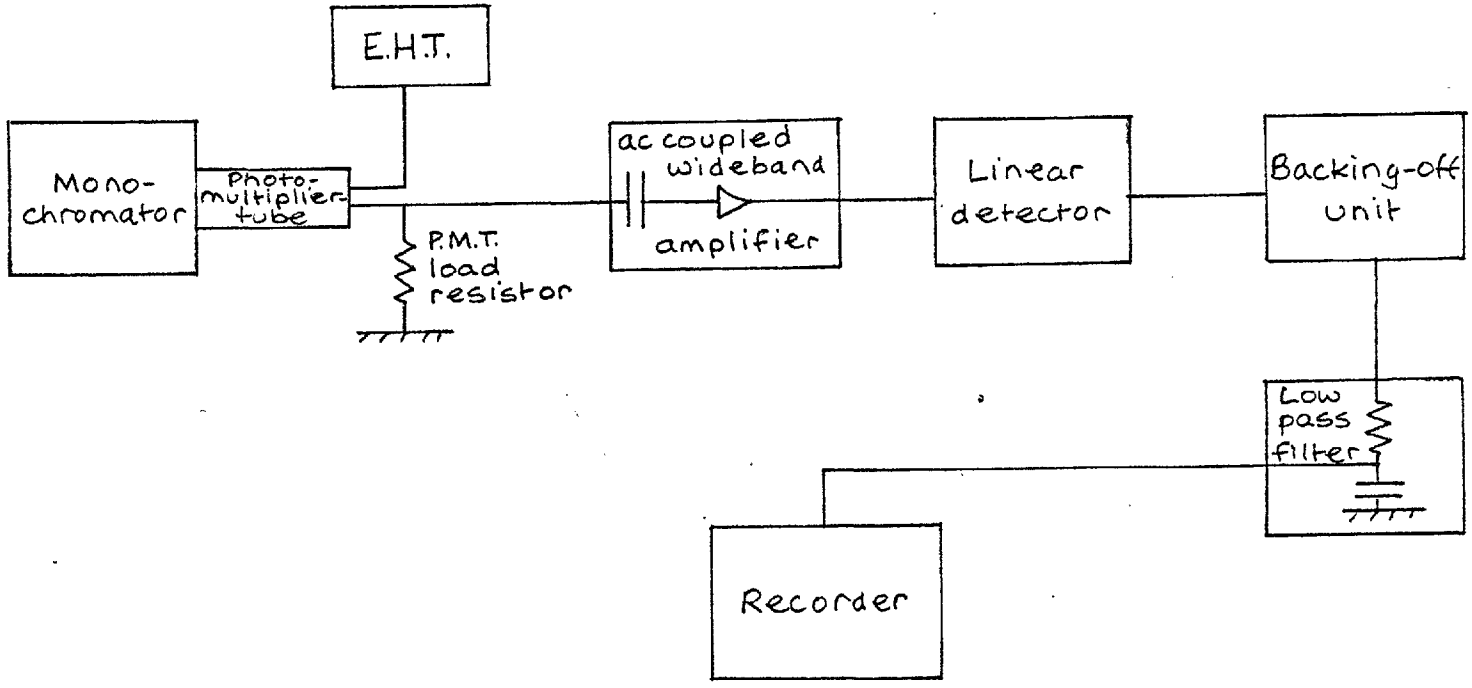

FIGURE 29

INSTRUMENTAL ASSEMBLY USING

NOISE-VOLTAGE DETECTION SYSTEM

indicated some of the practical solutions to those difficulties. There is no longer any doubt that analytical atomic spectroscopy is possible in the vacuum ultra-violet, and the possibility exists that the method may eventually encompass the entire periodic table.

REFERENCES

(1) A.Walsh . Spectrochim. Acta 7 108 (1955)

(2) B.J.Russell, J.P.Shelton and A.Walsh , Spectrochim. Acta 8 317 (1957)

(3) W.T.Elwell and J.A.F.Gidley . "Atomic Absorption Spectrophotometry" Pergamon, Oxford, 1960

(4) J.Ramirez-Muñoz . "Atomic Absorption Spectroscopy" Elsevier, London, 1968

(5) W.Slavin . "Atomic Absorption Spectroscopy" Interscience, London, 1968

(6) I.Rubeška and B.Moldan . "Atomic Absorption Spectrophotometry" Iliffe, London, 1969

(7) R.Mavrodineanu and H.Boiteux . "Flame Spectroscopy" Wiley, London, 1965

(8) A.C.G.Mitchell and M.W.Zemansky . "Resonance Radiation and Excited Atoms" University Press, Cambridge, 1934

(9) S.Tolansky . "High Resolution Spectroscopy" Methuen, London, 1947

(10) B.V.L'vov . "Atomic Absorption Spectrochemical Analysis" Adam Hilger, London,1970

(11) T.Lyman. "The Spectroscopy of the Extreme Ultra-Violet" Methuen, London, 1928

(12) J.A.R.Samson . "Techniques of Vacuum Ultra-Violet Spectroscopy" Wiley, London, 1967

(13) F.Paschen . Ann. Phys. 50 901 (1916)

(14) R.M.Dagnall, K.C.Thompson, and T.S.West . Talanta 14 551 (1967)

(15) J.H.McLeod . Phys. Rev. 45 802 (1934)

(16) B.V.L'vov . Spectrochim. Acta 24B 53 (1969)

(17) B.V.L'vov and G.G.Lebedev . Zh. Prikl. Spectroskopii 7 264 (1967)

(18) B.V.L'vov and A.D.Khartsyzov . Zh. Prikl. Spectroskopii 11 413 (1969)

(19) H.Massman . Spectrochim. Acta 23B 215 (1968)

(20) T.S.West and X.K.Williams . Anal. Chim. Acta 45 27 (1969)

(21) J.F.Alder and T.S.West . Anal. Chim. Acta 51 365 (1970)

(22) R.H.Wendt and V.A.Fassel . Anal. Chem. 38 337 (1966)

(23) G.F.Kirkbright, Analyst 96 609 (1971)

(24) J.E.Allan .Fourth Australian Spectroscopy Conference, August 1963

(25) R.M.Dagnall, K.C.Thompson and T.S.West. Atomic Ab. Nwsl. 6 117 (1967)

(26) A.Smithells and H.Ingle, J. Chem. Soc. 61 204 (1892)

(27) G.F.Kirkbright, M.Sargent and T.S.West. Talanta 16 1467 (1969)

(28) G.F.Kirkbright, M.K.Peters and T.S.West. Talanta 14 789 (1967)

(29) J.E.Chester, R.M.Dagnall and M.R.G.Taylor, Analyst 95 702 (1970)

(30) M.R.G.Taylor. Ph.D. Thesis, University of London, 1970

(31) G.F.Kirkbright and L.Ranson. Anal. Chem. 43 1238 (1971)

(32) W.L.Wiese, M.W.Smith and B.M.Miles. "Atomic Transition Probabilities" Vol. II, NSRDS - NBS22, National Bureau of Standards, Washington, D.C., U.S.A., 1969

(33) C.Candler. "Atomic Spectra and the Vector Model" Adam Hilger, London, 1964

(34) M.D.Amos, P.A.Bennet, K.G.Brodie, P.W.Y.Lung andJ.P.Matoušek. Anal. Chem. 43 211 (1971)

(35) H.E.Taylor, J.H.Gibson and R.K.Skogerboe, Anal. Chem. 42 1569 (1970)

(36) Hilger Journal IV(2) 19 (1957)

(37) Private communication, Messrs. Hilger and Watts Ltd., London

(38) D.C.Manning. Atomic Abs. Nwsl. 10 123 (1971)

(39) K.C.Thompson. Ph.D. Thesis, University of London, 1968

(40) G.F.Kirkbright, T.S.West and P.J.Wilson. Atomic Abs. Nwsl. 11 53 (1972)

(41) "IP Standards for Petroleum and its Products" Pts. I and II, Institute of Petroleum, London, 1970

(42) Machida Wataru, Okutani Tudao and Utsumi Satori. Bunseki Kagaku 17 1128 (1968) via Chem. Abs. 69 98169 (1968)

(43) E.V.Good, Analyst 93 663 (1968)

(44) F.C.A.Killer and K.E.Underhill. Analyst 95 505 (1970)

(45) ASTM, D2622-67, Part 17, 1971 Annual Book of ASTM Standards, American Society for Testing and Materials, Philadelphia, Pa, 1971

(46) R.J.Bird and R.W.Toft . J.Inst. Petroleum 56 170 (1970)
(47) C.Elejalde and F.Albisu . Ensayos Invest. 3 48 (1968)
(48) G.M.Hieftje -Anal. Chem. 44 (5) 81A (1972)
(49) C.T.Alkemade, H.P.Hoomayers, P.J.Lijnse and T.M.J.Vierbergen. Spectrochim. Acta 27B 149 (1972)
(50) P.C.Wildy and K.C.Thompson. Analyst 95 562 (1970)
(51) R.M.Dagnall, M.D.Sylvester and T.S.West . Talanta 18 1103 (1971)
(52) H.V.Malmstadt, M.L.Franklin and G.Horlick . Anal. Chem. 44 (8) 63A (1972)
(53) B.J.Sharp . Ph.D. Thesis, University of London, 1972
(54) G.A.Norton . Applied Optics 7 1 (1968)
(55) Elscint Scientific Instrumentation Catalogue GMD-10, 1972
(56) M.L.Franklin, G.Horlick and H.V.Malmstadt . Anal. Chem. 41 2 (1969)
(57) A.Walsh . Proc. of the X Colloquium Spectroscopicum Internationale, ppl3 - 26, Washington,1963
(58) D.C.Manning and Sabina Slavin . Atomic Abs. Nwsl. 8 132 (1969)
(59) F.A.Cotton and G.Wilkinson . "Advanced Inorganic Chemistry" 2nd Edition, Interscience, London, 1966
(60) P.Platt . "SAC Annual Reviews 1970" Society for Analytical Chemistry, London, 1970
(61) A.I.Bodretsova, B.V.L'vov, E.N.Pavlovskaya and V.K.Prokof'ev. Zh. Prikl. Spectroskopii 2 97 (1965)
(62) "Manual of Nutrition" Ministry of Agriculture, Fisheries and Food, H.M.S.O., London,1968
(63) A.R.Law, N.J.Nicholson and R.L.Norton . J.A.O.A.C. 54 (4) 764 (1971)
(64) G.F.Kirkbright and S.Vetter . Spectrochim. Acta 26B 505 (1971)
(65) M.L.Parsons, W.J.McCarthy and J.D.Winefordner. Applied Spectroscopy 20 223 (1966)
(66) R.F.Browner . Ph.D. Thesis, University of London, 1970
(67) I.Langmuir. Science 62 463 (1925)
(68) G.F.Kirkbright. Private communication
(69) G.F.Kirkbright, A.F.Ward and T.S.West. Anal. Chim. Acta (1973), in press

(70) G.F.Kirkbright, A.F.Ward and T.S.West, Anal. Chim. Acta (1973), in press

(71) G.F.Kirkbright, T.S.West and P.J.Wilson. Analyst (1973), in press

(72) P.M.Larkins, R.M.Lowe, J.V.Sullivan and A.Walsh, Spectrochim. Acta 24B 187 (1969)

(73) J.V.Sullivan and A.Walsh. Applied Optics 7 1271 (1968)

(74) R.R.Alfano and N.Ockman. J. Opt. Soc. America 58 90 (1968)